

A surprising observation on the quarter-plane diffraction problem

Raphael C. Assier* and I. David Abrahams†

* Department of Mathematics, University of Manchester, Oxford Road, Manchester, M13 9PL, UK

† Isaac Newton Institute, University of Cambridge, 20 Clarkson Road, Cambridge CB3 0EH, UK

9th January 2022

Abstract

In this paper, we revisit Radlow’s highly original attempt at a double Wiener–Hopf solution to the canonical problem of wave diffraction by a quarter-plane. Using a constructive approach, we reduce the problem to two equations, one containing his somewhat controversial ansatz, and an additional compatibility equation. We then show that despite Radlow’s ansatz being erroneous, it gives surprisingly accurate results in the far-field, in particular for the spherical diffraction coefficient. This unexpectedly good result is established by comparing it to results obtained by the recently established modified Smyshlyaev formulae.

1 Introduction

Since the middle of the twentieth century, the intrinsically three-dimensional canonical problem of wave diffraction by a quarter-plane has attracted a great deal of attention, with many different mathematical techniques employed in seeking useful solutions.

This diffraction problem, a natural extension to Sommerfeld’s famous half-plane problem [34, 35], represents one of the building blocks of the geometrical theory of diffraction (GTD, [18]). Its far-field behaviour is very rich, including a set of primary and secondary edge-diffracted waves as well as a spherical wave emanating from the corner of the quarter-plane. The primary and secondary edge waves can be described analytically using the GTD, see for example [7]. Other techniques such as ray asymptotic theory on a surface of a sphere [31] or a Sommerfeld-Malyuzhinets integral approach [21, 22] also lead to the same results. However, the spherical wave is more problematic. In particular, one of the remaining challenges is to obtain a simple (easy to evaluate) closed-form expression for its diffraction coefficient.

By considering the quarter-plane as a degenerated elliptic cone, the field can be expressed as a spherical wave multipole series involving Lamé functions [19, 28, 17]. However these series are poorly convergent in the far-field and as such cannot lead to the sought-after diffraction coefficient. A review of this approach and attempts to accelerate the series convergence are described in [13].

A different and more recent way of considering this problem, based on the use of spherical Green’s functions, has been introduced in [32, 33, 10] and led to an integral formula for the spherical diffraction coefficient. However, this solution is not valid for all incidence/observation directions and requires a numerical treatment and some regularisation of Abel-Poisson type in order for it to be evaluated [11].

Building on this type of approach, a hybrid numerical-analytical method, which partially solves the acoustic quarter-plane problem in the Dirichlet case has been introduced in [30, 29]. The main advantage of this method compared to the one mentioned previously is that in this case the formulae giving the diffraction coefficient, known as the *Modified Smyshlyaev Formulae* (MSF), are ‘naturally convergent’ in the sense that they do not require any special treatment to regularise or accelerate convergence. The method is based on planar and spherical edge Green’s functions and on the theory of *embedding formulae*, introduced in [38] and further developed in [16] for example. This method has been extensively described, adapted to the Neumann case and implemented in [6]. We will use this method as a benchmark in the present paper; its implementation relies on an *a priori* knowledge of the eigenvalues of the Laplace-Beltrami operator on a sphere with a slit. A detailed spectral analysis of this operator is given in [8]. In particular, it gives a rapid way of evaluating the diffraction coefficient for a wide range of incident wave and observer directions, but is not valid for all such directions. As discussed in [7], a reason behind the limits of the MSF validity is the existence of secondary edge-diffracted waves.

Another attempt, crucial to the present work, was published by Radlow in two successive papers [26, 27]. The method is based on a Wiener–Hopf [25, 20] approach in two complex variables, and the author obtains a closed-form solution in Fourier space. In the latter paper, an ansatz for the solution is proposed and a non-constructive intricate proof of its validity is given. This ansatz has long been known to be erroneous (see e.g. [24]), since it is shown to give the wrong tip behaviour. The correct tip behaviour should include an eigenvalue of the Laplace-Beltrami operator (see [15] for example). The technical reason as to why Radlow’s proof is incorrect has been given fairly recently in [3], in particular the field corresponding to his ansatz does not satisfy the correct boundary condition. For a more extensive literature review on the use of functions of two complex variables in diffraction theory, the reader can be referred to the introduction of [9].

In the present work, we revisit Radlow’s approach and offer a formally exact solution from which we show that his ansatz appears constructively in a natural way. However, there is an extra term, which proves that Radlow’s ansatz cannot be the true solution. The extra term is complicated, and contains integrals of as-yet unknown functions. The calculation/approximation of this term will be the subject of future work. However, while doing this work, we came across what we can refer to as a *surprising observation*. Serendipity made us compare the spherical diffraction coefficient calculated with Radlow’s ansatz, i.e. setting the additional term to zero, to the one calculated using the MSF approach. It turns out, as we will show, that the two are very close (at least in the Dirichlet case). Some hints can be found in the literature regarding the accuracy of Radlow’s ansatz compared to full numerical computations [4, 36], though, never before were the diffraction coefficients compared like for like.

In Section 2, the problem is formulated, and symmetries are exploited. In Section 3, the machinery required to work in Fourier space for two complex variables is introduced, the Wiener-Hopf functional equation is derived, and the inverse transform form of the solution is written down. Throughout this work, and starting from this section, we will use the phase portrait technique (see [37]) to visualise functions of a complex variable. This visualisation technique will play an important role in our reasoning. In Section 4, we present a way of factorising the Wiener-Hopf kernel into four factors with known analyticity properties. We write each factor as a modified Cauchy integral, in the form that allows easy implementation and fast evaluation. In Section 5, two successive Wiener-Hopf procedures are performed, leading to the theoretical core of the present work: the two equations (5.12)–(5.13) linking the main unknowns of the problem. The first equation involves Radlow’s ansatz and an additional term, while the second equation, which we call the *compatibility equation*, may provide a way to find the unknown additional term. The

diffraction coefficient is related to the solution of the Wiener-Hopf problem. Finally, in Section 6, we compare the diffraction coefficient obtained by the MSF technique to that obtained assuming that Radlow's ansatz is correct. As we shall show, the two are surprisingly in very close agreement.

2 Formulation

2.1 Geometry, governing equation and incident wave

Let us consider the three-dimensional (x_1, x_2, x_3) space, and the quarter plane QP defined by

$$\text{QP} = \{\mathbf{x} = (x_1, x_2, x_3) \in \mathbb{R}^3, \text{ such that } x_1 \geq 0, x_2 \geq 0 \text{ and } x_3 = 0\}, \quad (2.1)$$

and illustrated in Figure 1. We aim to solve the three-dimensional wave equation

$$\frac{\partial^2 \mathbf{u}_{\text{tot}}}{\partial t^2} = c^2 \Delta \mathbf{u}_{\text{tot}} \text{ and } \frac{\partial^2 \mathbf{u}}{\partial t^2} = c^2 \Delta \mathbf{u}, \quad (2.2)$$

in $\mathbb{R}^3 \setminus \text{QP}$ for the total velocity potential \mathbf{u}_{tot} and the scattered velocity potential \mathbf{u} , when the quarter-plane is subject to an incident plane wave $\mathbf{u}_{\text{in}} = e^{i(\mathbf{k} \cdot \mathbf{x} - \Omega t)}$, so that we can write $\mathbf{u}_{\text{tot}} = \mathbf{u}_{\text{in}} + \mathbf{u}$. Ω represents the radian frequency of the incident wave, c is the speed of sound and \mathbf{k} is the incident wavevector, such that the wavenumber $k = |\mathbf{k}|$ is given by $k = \Omega/c$. To be consistent with Radlow, we take the total field to satisfy the Dirichlet (soft) boundary condition $\mathbf{u}_{\text{tot}} = 0$ on QP. As is usual in scattering problems, let us make the hypothesis of time-harmonicity, assuming that all time-dependent quantities involved have a time-dependency consisting solely in a multiplicative factor $e^{-i\Omega t}$. We can then introduce the quantities $u_{\text{tot}}(\mathbf{x})$, $u_{\text{in}}(\mathbf{x})$ and $u(\mathbf{x})$, defined by $\mathbf{u}_{\text{tot}}(\mathbf{x}, t) = \text{Re}(u_{\text{tot}}(\mathbf{x})e^{-i\Omega t})$, $\mathbf{u}_{\text{in}}(\mathbf{x}, t) = \text{Re}(u_{\text{in}}(\mathbf{x})e^{-i\Omega t})$ and $\mathbf{u}(\mathbf{x}, t) = \text{Re}(u(\mathbf{x})e^{-i\Omega t})$ respectively. As a consequence, the total field $u_{\text{tot}}(\mathbf{x})$ and the scattered field u should satisfy the Helmholtz equation

$$\Delta u + k^2 u = 0 \text{ on } \mathbb{R}^3 \setminus \text{QP} \quad (2.3)$$

and u_{tot} should satisfy the Dirichlet boundary condition

$$u_{\text{tot}} = 0 \text{ on QP}. \quad (2.4)$$

The wavevector \mathbf{k} is oriented in the incident direction towards the vertex of the quarter-plane (also the origin of our three-dimensional space) and as such, we can write $\mathbf{k} = -k\boldsymbol{\omega}_0$, where $\boldsymbol{\omega}_0$ represents the point of the unit sphere determining the incident direction. Using the spherical coordinates (r, θ, φ) , as illustrated in Figure 1, we can introduce θ_0 and φ_0 , such that $\boldsymbol{\omega}_0$ corresponds to the point with spherical coordinates $(1, \theta_0, \varphi_0)$ and hence $\boldsymbol{\omega}_0$ can be represented in Cartesian coordinates by $(\sin(\theta_0) \cos(\varphi_0), \sin(\theta_0) \sin(\varphi_0), \cos(\theta_0))$.

The incident wave can hence be rewritten as

$$u_{\text{in}}(\mathbf{x}) = e^{i\mathbf{k} \cdot \mathbf{x}} = e^{-ik\boldsymbol{\omega}_0 \cdot \mathbf{x}} = e^{-i(a_1 x_1 + a_2 x_2 + a_3 x_3)}, \quad (2.5)$$

where $a_1 = k \sin(\theta_0) \cos(\varphi_0)$, $a_2 = k \sin(\theta_0) \sin(\varphi_0)$ and $a_3 = k \cos(\theta_0)$.

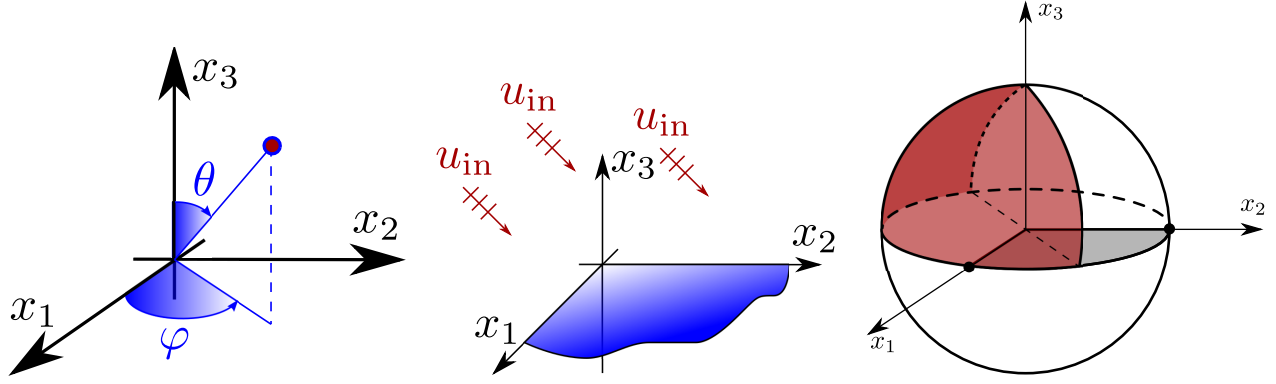


Figure 1: Spherical coordinates definition, quarter-plane illustration and geometric restriction of incidence

2.2 Edge, vertex and radiation conditions

In order for the problem to be well-posed, some other conditions need to be satisfied. These have been dealt with in detail in [8] for example, and so we will be brief. We impose the edge and vertex conditions: the energy of the field should remain bounded as we approach the edges and the vertex (i.e. no sources should be located on these), and the radiation condition: the scattered field u should be outgoing in the far-field (i.e. no sources other than the incident wave at infinity).

2.3 Symmetries of the problem

Let us now exploit the symmetry of the problem in order to reduce the range of the incident wave. First of all, due to the obvious “vertical symmetry” of the quarter-plane, it is enough to restrict the problem to incident waves coming from above the quarter-plane; this means that θ_0 lies within $[0, \pi/2]$. Moreover, in the (x_1, x_2) -plane, our domain is symmetric with respect to the bisector separating the quarter-plane into two plane sector with internal angle $\pi/4$; i.e. it is possible to restrict φ_0 to belong to $[-3\pi/4, \pi/4]$, corresponding to the restricted zone of incidence depicted in Figure 1.

Finally, it is well-known that the scattered field u is symmetric (this can be seen by decomposing the field into its symmetric and antisymmetric parts), i.e., we have $u(x_1, x_2, x_3) = u(x_1, x_2, -x_3)$. Note that this automatically implies that $\partial u / \partial x_3$ is an antisymmetric function. Therefore we can also restrict the observer region to $x_3 \geq 0$, i.e. $\theta \in [0, \pi/2]$.

2.4 Jump in normal derivative across the quarter-plane

Let us consider the quantity

$$f(x_1, x_2) = \left[\frac{\partial u}{\partial x_3} \right]_{x_3=0^-}^{x_3=0^+} = \frac{\partial u}{\partial x_3}(x_1, x_2, 0^+) - \frac{\partial u}{\partial x_3}(x_1, x_2, 0^-).$$

It is clear that in the part of the $x_3 = 0$ plane that does not contain QP, this quantity should be zero, since u and its normal derivative are continuous. So we have that $f(x_1 < 0, x_2) = f(x_1, x_2 < 0) = 0$.

On QP, the far-field will be of the form $u = u_{\text{re}} + u_{\text{diff}}$ on the (top) illuminated face, while it will be of the form $u = -u_{\text{in}} + u_{\text{diff}}$ on the bottom face. Here u_{re} represents the reflected wave and is given by $u_{\text{re}}(x_1, x_2, x_3) = -e^{-i(a_1 x_1 + a_2 x_2 - a_3 x_3)}$, and u_{diff} encompasses all the different diffracted

fields (primary and secondary edge diffraction plus corner diffraction), which decay at least like $1/\sqrt{k\rho}$, where ρ is the distance to the closest edge. Hence as both x_1 and x_2 tend to $+\infty$, we will have $u \sim u_{\text{re}}$ on the illuminated face and $u \sim -u_{\text{in}}$ on the bottom face. Hence we have

$$f(x_1, x_2) \underset{x_1, x_2 \rightarrow +\infty}{\sim} \frac{\partial u_{\text{re}}}{\partial x_3}(x_1, x_2, 0^+) + \frac{\partial u_{\text{in}}}{\partial x_3}(x_1, x_2, 0^-) \underset{x_1, x_2 \rightarrow +\infty}{=} \mathcal{O}(e^{-i(a_1 x_1 + a_2 x_2)}).$$

2.5 Formulation summary

To summarise, the scattering problem we wish to solve is the following:

$$\begin{aligned} u_{\text{tot}}(\mathbf{x}) &= u_{\text{in}}(\mathbf{x}) + u(\mathbf{x}), \quad u_{\text{in}}(\mathbf{x}) = e^{-i(a_1 x_1 + a_2 x_2 + a_3 x_3)}, \\ \Delta u + k^2 u &= 0 \text{ on } \mathbb{R}^3 \setminus \text{QP}, \quad u_{\text{tot}}(\mathbf{x}) = 0 \text{ on QP}, \\ f(x_1, x_2) &\underset{x_1, 2 \rightarrow \infty}{=} \mathcal{O}(e^{-i(a_1 x_1 + a_2 x_2)}) \end{aligned} \tag{2.6}$$

$$f(x_1, x_2) = 0 \text{ for } (x_1, x_2) \in Q_2 \cup Q_3 \cup Q_4, \tag{2.7}$$

subject to the vertex, edge and radiation conditions. The Q_i are the different quadrants of the equatorial (x_1, x_2) -plane, illustrated in Figure 2, and defined by

$$\begin{aligned} Q_1 &= \{(x_1, x_2), x_1 \geq 0 \text{ and } x_2 \geq 0\}, \quad Q_2 = \{(x_1, x_2), x_1 \leq 0 \text{ and } x_2 \geq 0\}, \\ Q_3 &= \{(x_1, x_2), x_1 \leq 0 \text{ and } x_2 \leq 0\}, \quad Q_4 = \{(x_1, x_2), x_1 \geq 0 \text{ and } x_2 \leq 0\}. \end{aligned}$$

It is convenient at this point to defer the solution of this boundary value problem to Sections 5 and 6. In the following Sections, 3 and 4, it will be helpful to the general reader to first introduce the mathematical machinery to be employed later. This will, of necessity, be rather tedious; hence, a more experienced reader may choose to start with Section 5 and refer back to the earlier sections as required.

3 Transformation in Fourier space

3.1 Some useful functions

In order to be able to define precisely quantities of interest in the following section, we need to introduce a few intermediate functions, as well as some useful notations. Let $\log(z)$ and \sqrt{z} be the default complex logarithm and square root used by most mathematical software (e.g. Mathematica, Matlab, etc.). They correspond to the usual principal value of the logarithm and square root on the positive real axis and have a branch cut on the negative real axis. Let us now define a slightly different version of the logarithm: the function $\overset{\swarrow}{\log}$, that will be used first in Section 4.2.2, defined by $\overset{\swarrow}{\log}(z) = \log\left(e^{-\frac{i\pi}{4}} z\right) + \frac{i\pi}{4}$, so that this is a logarithm in the sense that $\exp(\overset{\swarrow}{\log}(z)) = z$, it coincides with the usual real logarithm on the positive real axis, and has a branch cut extending diagonally down from the branch point $z = 0$, as illustrated in Figure 2.

Let us now define the function $\overset{\swarrow}{\sqrt{z}}$, that will be used extensively throughout this work, by $\overset{\swarrow}{\sqrt{z}} = e^{i\frac{\pi}{4}} \sqrt{-iz}$ so that this is a square root in the sense that $(\overset{\swarrow}{\sqrt{z}})^2 = z$, it coincides with the usual real square root on the positive real axis, and has a branch cut on the negative imaginary

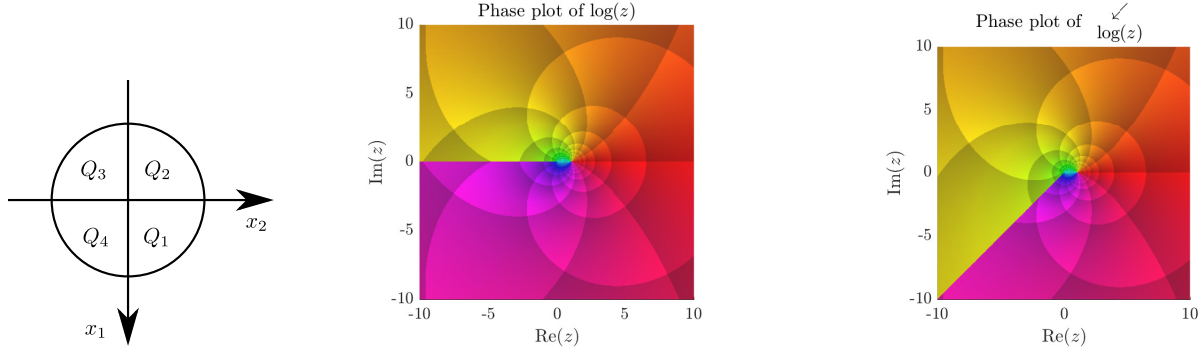


Figure 2: The quadrants Q_i and phase portraits of the functions $\log(z)$ and $\check{\log}(z)$

axis, as shown in Figure 3. Building on this, we can define the function $\kappa(\mathfrak{K}, z)$ for any \mathfrak{K} such that $\text{Im}(\mathfrak{K}) \geq 0$ and $\text{Re}(\mathfrak{K}) > 0$ by

$$\kappa(\mathfrak{K}, z) = \sqrt[4]{\mathfrak{K} - z} \sqrt[4]{\mathfrak{K} + z}. \quad (3.1)$$

The function κ satisfies $(\kappa(\mathfrak{K}, z))^2 = \mathfrak{K}^2 - z^2$ with the principal Riemann sheet chosen such that $\kappa(\mathfrak{K}, 0) = \mathfrak{K}$. It has two branch cuts in the complex z plane, one starting at the branch point $z = \mathfrak{K}$ and extending vertically upwards, and one starting at the branch point $z = -\mathfrak{K}$ and extending vertically downwards¹ as can be visualised in Figure 3.

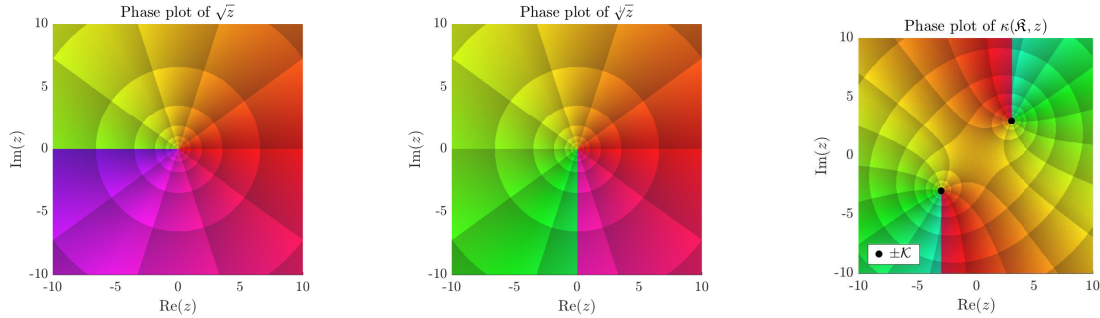


Figure 3: Phase portraits of the three functions \sqrt{z} , $\sqrt[4]{z}$, and $\kappa(\mathfrak{K}, z)$ for $\mathfrak{K} = 3 + 3i$.

In the rest of the paper, we will sometimes use the bold notation α to represent the two variables (α_1, α_2) . Let us now define the function $K(\alpha)$ as follows:

$$K(\alpha_1, \alpha_2) = \frac{1}{\kappa(\kappa(k, \alpha_2), \alpha_1)}, \quad (3.2)$$

such that we have

$$(K(\alpha))^2 = \frac{1}{(\kappa(\kappa(k, \alpha_2), \alpha_1))^2} = \frac{1}{(\kappa(k, \alpha_2))^2 - \alpha_1^2} = \frac{1}{k^2 - \alpha_2^2 - \alpha_1^2}$$

¹The arrow notations used throughout this paper have the main objective of giving the reader an easy way to implement this work on a computer. One should also note that even if κ is defined with two down-arrow functions, one of its branches is vertical upwards. This is due to the fact that the argument within one of the down-arrow function is $-z$.

and define the function $\gamma(\boldsymbol{\alpha})$ as

$$\gamma(\boldsymbol{\alpha}) = -i/K(\boldsymbol{\alpha}) \text{ such that } (\gamma(\boldsymbol{\alpha}))^2 = \alpha_1^2 + \alpha_2^2 - k^2. \quad (3.3)$$

Note that, by definition of κ , we have $1/K(0,0) = k$ and $\gamma(0,0) = -ik$.

3.2 Double Fourier transform representation

Let us now apply the double Fourier transform (denoted by the operator \mathfrak{F}) in the (x_1, x_2) directions. Let us call $U(\alpha_1, \alpha_2, x_3)$ the double Fourier transform of $u(x_1, x_2, x_3)$, such that we have

$$\begin{aligned} U(\alpha_1, \alpha_2, x_3) &= \mathfrak{F}[u] = \int_{-\infty}^{\infty} \int_{-\infty}^{\infty} u(x_1, x_2, x_3) e^{i(\alpha_1 x_1 + \alpha_2 x_2)} dx_2 dx_1, \\ u(x_1, x_2, x_3) &= \mathfrak{F}^{-1}[U] = \frac{1}{(2\pi)^2} \int_{\mathcal{A}_1} \int_{\mathcal{A}_2} U(\alpha_1, \alpha_2, x_3) e^{-i(\alpha_1 x_1 + \alpha_2 x_2)} d\alpha_2 d\alpha_1. \end{aligned}$$

The contours of integration \mathcal{A}_1 and \mathcal{A}_2 in the inverse transform will in general not completely lie on the real line, but will start at $-\infty$ and end at $+\infty$. An exact description will be given in Section 3.3.1. Under this double Fourier transformation, the Helmholtz equation is changed into $(-\alpha_1^2 - \alpha_2^2)U + \frac{\partial^2 U}{\partial x_3^2} + k^2 U = 0$, which can be rewritten as

$$\frac{\partial^2 U}{\partial x_3^2} - \gamma^2(\boldsymbol{\alpha})U = 0, \text{ where, as already stated, } \gamma^2(\boldsymbol{\alpha}) = \alpha_1^2 + \alpha_2^2 - k^2. \quad (3.4)$$

The contours \mathcal{A}_1 and \mathcal{A}_2 will be chosen later such that $\text{Re}(\gamma(\boldsymbol{\alpha})) \geq 0$ when $\boldsymbol{\alpha} \in \mathcal{A}_1 \times \mathcal{A}_2$. Hence in order not to have exponential growth as x_3 tends to infinity, and because $x_3 \geq 0$, we must have

$$U(\boldsymbol{\alpha}, x_3) = G(\boldsymbol{\alpha}) e^{-\gamma(\boldsymbol{\alpha})x_3}. \quad (3.5)$$

Hence, we can write $u(\mathbf{x})$ using the inverse Fourier representation

$$u(\mathbf{x}) = \frac{1}{(2\pi)^2} \int_{\mathcal{A}_1} \int_{\mathcal{A}_2} G(\alpha_1, \alpha_2) e^{-i(\alpha_1 x_1 + \alpha_2 x_2)} e^{-\gamma(\alpha_1, \alpha_2)x_3} d\alpha_2 d\alpha_1. \quad (3.6)$$

We can write $f(x_1, x_2)$ in a similar fashion, using the symmetry of the solution (see Section 2.3):

$$f(x_1, x_2) = 2 \frac{\partial u}{\partial x_3}(x_1, x_2, 0^+) = \frac{-2}{(2\pi)^2} \int_{\mathcal{A}_1} \int_{\mathcal{A}_2} \gamma(\boldsymbol{\alpha}) G(\boldsymbol{\alpha}) e^{-i(\alpha_1 x_1 + \alpha_2 x_2)} d\alpha_2 d\alpha_1 \quad (3.7)$$

Hence, upon introducing $F(\boldsymbol{\alpha})$ defined by

$$F(\boldsymbol{\alpha}) = -2\gamma(\boldsymbol{\alpha})G(\boldsymbol{\alpha}), \quad (3.8)$$

the equation (3.7) becomes

$$f(x_1, x_2) = \frac{1}{(2\pi)^2} \int_{\mathcal{A}_1} \int_{\mathcal{A}_2} F(\boldsymbol{\alpha}) e^{-i(\alpha_1 x_1 + \alpha_2 x_2)} d\alpha_2 d\alpha_1,$$

which means that the function F introduced in (3.8) is in fact the double Fourier transform of f , i.e.

$$F(\alpha_1, \alpha_2) = \int_{-\infty}^{\infty} \int_{-\infty}^{\infty} f(x_1, x_2) e^{i(\alpha_1 x_1 + \alpha_2 x_2)} dx_2 dx_1. \quad (3.9)$$

In what follows, it will be convenient to use K instead of γ and rewrite (3.8) as

$$G(\boldsymbol{\alpha}) = \frac{1}{2i} F(\boldsymbol{\alpha}) K(\boldsymbol{\alpha}), \quad (3.10)$$

which is the most important *functional equation*² of the problem. It relates the Fourier transform of u and $\frac{\partial u}{\partial x_3}$ at $x_3 = 0^+$ and will be exploited to obtain the main result of the paper: equations (5.12)–(5.13). Using (3.10) in (3.8) the wave field u is given by

$$u(\mathbf{x}) = \frac{1}{(2\pi)^2} \int_{\mathcal{A}_1} \int_{\mathcal{A}_2} \frac{F(\boldsymbol{\alpha}) K(\boldsymbol{\alpha})}{2i} e^{-i(\alpha_1 x_1 + \alpha_2 x_2)} e^{i \frac{x_3}{K(\boldsymbol{\alpha})}} d\alpha_2 d\alpha_1. \quad (3.11)$$

3.3 A small departure from the usual approach

As is usually the case when using the Wiener-Hopf technique, we could start by assuming that k has a small positive imaginary part. Following this approach, it is possible to show that there exist four real numbers b_1, δ_1, b_2 and δ_2 , with $b_1 < \delta_1$ and $b_2 < \delta_2$, such that the function of interest $F(\boldsymbol{\alpha}) K(\boldsymbol{\alpha})$ is analytic on the tubular domain $\mathcal{D}^* \subset \mathbb{C}^2$ defined by $\mathcal{D}^*(b_1, b_2, \delta_1, \delta_2) = \mathcal{S}(b_1, \delta_1) \times \mathcal{S}(b_2, \delta_2)$, where for two real numbers $b < \delta$, the strip $\mathcal{S}(b, \delta) \subset \mathbb{C}$ is defined by $\mathcal{S}(b, \delta) = \{z \in \mathbb{C}, b < \text{Im}(z) < \delta\}$. In fact, it is possible to get an explicit expression for $\delta_{1,2}$ and $b_{1,2}$:

$$\delta_1 = \text{Im}(k) |\cos(\varphi_0)|, \delta_2 = \text{Im}(k) |\sin(\varphi_0)|, b_{1,2} = \max(-\delta_{1,2}, \text{Im}(a_{1,2})). \quad (3.12)$$

However, if we want the solution for real k , the strips shrink to the real axes, and indented contours are needed in order to evaluate the inverse Fourier transforms. Our approach here, in the spirit of [1], will be to start directly from such indented contours and avoid the limiting procedure discussion that would be required with the usual approach. We want to choose two contours \mathcal{A}_1 and \mathcal{A}_2 in the α_1 and α_2 complex planes such that:

- (i) For any $\alpha_1^* \in \mathcal{A}_1$, the functions $F(\alpha_1^*, \cdot)$ and $K(\alpha_1^*, \cdot)$ are analytic on \mathcal{A}_2 .
- (ii) For any $\alpha_2^* \in \mathcal{A}_2$, the functions $F(\cdot, \alpha_2^*)$ and $K(\cdot, \alpha_2^*)$ are analytic on \mathcal{A}_1 .
- (iii) \mathcal{A}_1 and \mathcal{A}_2 are smooth contours starting at $-\infty$ and finishing at $+\infty$.
- (iv) For simplicity we would prefer that \mathcal{A}_1 be independent of α_2 and \mathcal{A}_2 be independent of α_1 .
- (v) For any $\boldsymbol{\alpha} \in \mathcal{A}_1 \times \mathcal{A}_2$, $\text{Re}(\gamma(\boldsymbol{\alpha})) = \text{Im}(1/K(\boldsymbol{\alpha})) \geq 0$.

3.3.1 On fulfilling the requirements (i)–(v) for $K(\boldsymbol{\alpha})$

In this subsection, we will show that there exist contours \mathcal{A}_1 and \mathcal{A}_2 that fulfil all the previous requirements (i)–(v) relative to the function $K(\boldsymbol{\alpha})$. Remember that $K(\boldsymbol{\alpha})$ is defined by $1/\kappa(\kappa(k, \alpha_2), \alpha_1)$, and that by this definition (which breaks the symmetry between α_1 and α_2), K does not behave in the same way in the α_1 plane and in the α_2 plane. In other words, even if by definition we have $K^2(\alpha_1, \alpha_2) \equiv K^2(\alpha_2, \alpha_1)$, we will not necessarily have $K(\alpha_1, \alpha_2) = K(\alpha_2, \alpha_1)$ for every $(\alpha_1, \alpha_2) \in \mathbb{C}^2$.

To be more precise, for a fixed α_2^* such that $\text{Im}(\kappa(k, \alpha_2^*)) \geq 0$, we expect the function $K(\alpha_1, \alpha_2^*)$ to simply have two branch points at $\pm \kappa(k, \alpha_2^*)$, with branch cuts extending vertically up and down,

²An alternative derivation, based on Green's identity, is given in [9].

respectively, in the α_1 complex plane, see Figure 4 (left). Hence, a suitable contour \mathcal{A}_1 would lie on the real line indented above $-\kappa(k, \alpha_2^*)$ and below $\kappa(k, \alpha_2^*)$ for any $\alpha_2^* \in \mathcal{A}_2$.

If we now fix an α_1^* and consider the function $K(\alpha_1^*, \alpha_2)$, we expect the analyticity structure to be a bit more complicated in the α_2 plane. In particular, we expect to have potential problems at $\alpha_2 = \pm k$ due to the term $\kappa(k, \alpha_2)$, perhaps leading to a branch cut extending vertically upwards from $\pm k$. However, we also expect to have branch points where $\kappa(k, \alpha_2) = \pm\alpha_1^*$, i.e., points where $\alpha_2 = \pm\kappa(k, \alpha_1^*)$, see Figure 4 (right). Hence, a suitable contour \mathcal{A}_2 would pass above $-k$ and $-\kappa(k, \alpha_1^*)$ and below k and $\kappa(k, \alpha_1^*)$ for any $\alpha_1^* \in \mathcal{A}_1$.

If, as mentioned previously, it is possible to prove rigorously that some contours are valid in the case when k has a small positive imaginary part, it is much harder to do so for real k . Instead, we will provide a *visual proof* that a given choice of \mathcal{A}_1 and \mathcal{A}_2 is suitable. Let us then consider the contours \mathcal{A}_1 and \mathcal{A}_2 to be smoothly passing above $-k$ and below k and also passing through the origins of their respective complex planes. A practical realisation of such contours can be obtained by the parametrisation $\mathcal{A}_1(s_1) = s_1 + \frac{s_1}{a(s_1^4+c)}$ and $\mathcal{A}_2(s_2) = s_2 + \frac{s_2}{a(s_2^4+c)}$, for $s_{1,2} \in \mathbb{R}$ and some complex constants a and c . As such \mathcal{A}_1 and \mathcal{A}_2 satisfy (iii)-(iv).

Given such a choice, it is possible to plot the loci of points $\pm\kappa(k, \mathcal{A}_2)$ in the α_1 plane and the loci $\pm\kappa(k, \mathcal{A}_1)$ in the α_2 plane. As long as our contours do not intersect these curves and do not intersect any resultant branch cuts, they should be valid. In fact, this can be seen in Figure 4, where the phase plots of $K(\alpha_1, \alpha_2^*)$ and $K(\alpha_1^*, \alpha_2)$ are shown for different values of $\alpha_1^* \in \mathcal{A}_1$ and $\alpha_2^* \in \mathcal{A}_2$, together with the loci mentioned above.

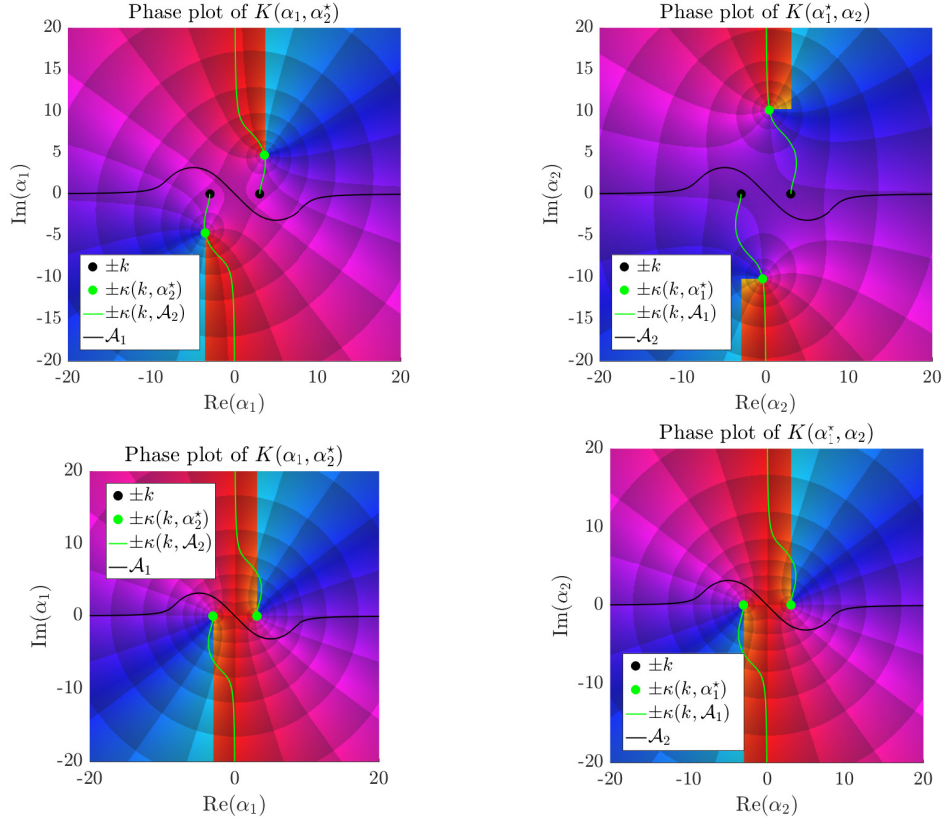


Figure 4: **(Visual proof of analyticity)** Visualisation of K in the α_1 plane (left: $\alpha_2^* = \mathcal{A}_2(5)$ (top) and $\alpha_2^* = \mathcal{A}_2(0)$ (bottom)) and in the α_2 plane (right: $\alpha_1^* = \mathcal{A}_1(10)$ (top) and $\alpha_1^* = \mathcal{A}_1(0)$ (bottom)). Here and in Figure 5 we chose $k = 3$, $a = 0.0012 + 0.0006i$ and $c = 1000i$.

As one can infer from Figure 4, the contours \mathcal{A}_1 and \mathcal{A}_2 , chosen suitably, avoid the singularities of K . In other words, for any $\alpha_2^* \in \mathcal{A}_2$, the function $K(\alpha_1, \alpha_2^*)$ is analytic on \mathcal{A}_1 , while for any $\alpha_1^* \in \mathcal{A}_1$, the function $K(\alpha_1^*, \alpha_2)$ is analytic on \mathcal{A}_2 . Hence, as far as K is concerned, this choice satisfies the conditions (i)–(iv). We still need to check that the condition (v) is satisfied. Again, here we will use a *visual approach*. The phase portrait of $\text{Im}(1/K(\alpha_1, \alpha_2^*))$ and $\text{Im}(1/K(\alpha_1^*, \alpha_2))$ for different values of $\alpha_1^* \in \mathcal{A}_1$ and $\alpha_2^* \in \mathcal{A}_2$ are displayed in Figure 5. The regions where $\text{Im}(1/K) > 0$ appear in red, while those where $\text{Im}(1/K) < 0$ appear in blue.

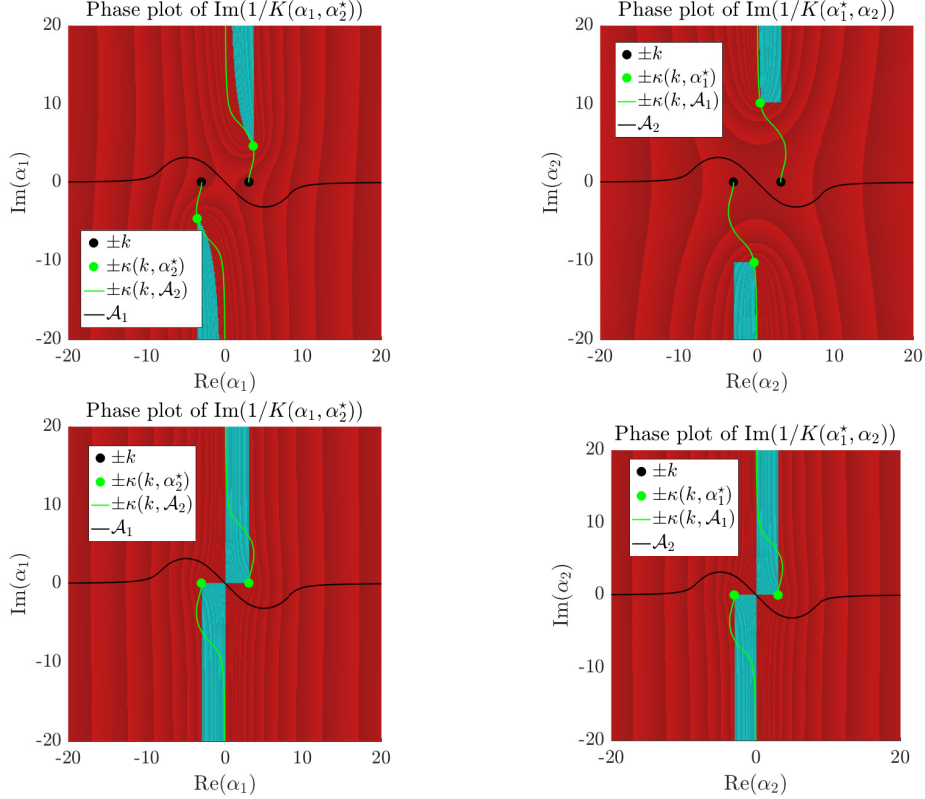


Figure 5: **(Visual proof of sign compatibility)** Visualisation of $\text{Im}(1/K)$ in the α_1 plane (left: $\alpha_2^* = \mathcal{A}_2(5)$ (top) and $\alpha_2^* = \mathcal{A}_2(0)$ (bottom)) and in the α_2 plane (right: $\alpha_1^* = \mathcal{A}_1(10)$ (top) and $\alpha_1^* = \mathcal{A}_1(0)$ (bottom)). The region where $\text{Im}(1/K) \geq 0$ appears in red on the plots.

As one can infer from Figure 5, for any $\alpha \in \mathcal{A}_1 \times \mathcal{A}_2$, we have $\text{Im}(1/K(\alpha)) \geq 0$, as required in order for (v) to be satisfied. Note also that it only becomes zero when both α_1 and α_2 are zero. It also shows that if \mathcal{A}_1 is chosen as above, \mathcal{A}_2 is forced to pass through the origin, and vice-versa.

3.3.2 On fulfilling the requirements (i)–(ii) for $F(\alpha)$

Remember that F is defined in (3.9), and so using the condition (2.7), it reduces to

$$F(\alpha_1, \alpha_2) = \int_0^\infty \int_0^\infty f(x_1, x_2) e^{i(\alpha_1 x_1 + \alpha_2 x_2)} dx_2 dx_1. \quad (3.13)$$

In order to understand the analyticity property of F , we need to use the following lemma.

Lemma 3.1 *Let $\phi(x_1, x_2)$ be a function of the two real variables x_1 and x_2 and let $\gamma_1, \gamma_2 \in \mathbb{R}$ be such that $|\phi(x_1, x_2)| \leq A_1 \exp(\gamma_1 x_1 + \gamma_2 x_2)$ as $|x_1| \rightarrow \infty$ and $|x_2| \rightarrow \infty$ and $(x_1, x_2) \in Q_1$. Then the function $\Phi(\alpha_1, \alpha_2)$ defined by*

$$\Phi(\alpha_1, \alpha_2) = \int_0^\infty \int_0^\infty \phi(x_1, x_2) e^{i(\alpha_1 x_1 + \alpha_2 x_2)} dx_2 dx_1$$

can be interpreted as a function of the complex variable $\alpha \in \mathbb{C}^2$, and as such, it is analytic in $\text{UHP}(\gamma_1) \times \text{UHP}(\gamma_2)$ considered an open subset of \mathbb{C}^2 , where the upper-half plane $\text{UHP}(\gamma_{1,2})$ is the region in the $\alpha_{1,2}$ complex plane lying above the horizontal line $\text{Im}(\alpha_{1,2}) = \gamma_{1,2}$.

In our case, because of the estimate (2.6), we can show that there exists $M > 0$, such that $|f(x_1, x_2)| \leq M \exp(\text{Im}(a_1)x_1 + \text{Im}(a_2)x_2)$ as $x_1, x_2 \rightarrow \infty$ within Q_1 , where $a_{1,2}$ are related to the incident wave direction as defined below (2.5). Moreover, since k is considered real, $\text{Im}(a_{1,2}) = 0$. Hence, in the notation of Lemma 3.1, we have $\gamma_{1,2} = 0$ and we can conclude that F is analytic on $\text{UHP}(0) \times \text{UHP}(0)$, i.e, for $\text{Im}(\alpha_{1,2}) > 0$.

However, this does not mean that F cannot be analytically continued onto a bigger domain. This realisation is important since the contours \mathcal{A}_1 and \mathcal{A}_2 defined in Section 3.3.1 do not lie within $\text{UHP}(0) \times \text{UHP}(0)$ since they both drop under their respective real axes.

Hence, let us try to infer *a priori*³ a bit more about the behaviour of F outside $\text{UHP}(0) \times \text{UHP}(0)$. First of all, the estimate (2.6), giving the behaviour of $f(x_1, x_2)$ at infinity gives us some information about the behaviour of $F(\alpha)$ within a finite part of the complex planes. Namely, we can expect that $F(\alpha_1, \alpha_2)$ will have a simple pole in the α_1 plane at $\alpha_1 = a_1$ and a simple pole in the α_2 plane at $\alpha_2 = a_2$. It also seems reasonable to expect that other possible singular behaviours would occur in the lower-half planes, e.g. branch points at $-k$ and maybe also on $-\kappa(k, \mathcal{A}_{1,2})$ and at $-\kappa(k, a_{1,2})$, once $\mathcal{A}_{1,2}$ have been specified.

Therefore, if a_1 and a_2 are negative, the contours \mathcal{A}_1 and \mathcal{A}_2 will be appropriate, since they are passing above the poles and the possible singular parts of F .

Remark 3.1 The situation is different if $a_{1,2}$ is positive, as then the contours $\mathcal{A}_{1,2}$ shown in Figure 4 will pass below the pole. A simple way to overcome what is a technical difficulty is to allow $a_{1,2}$ to have a small imaginary part $\epsilon < 0$ say, when $\text{Re}(a_{1,2}) > 0$. Then one can choose the contour $\mathcal{A}_{1,2}$ to lie sufficiently close to the real line that it passes above the pole, and the pole itself is located so that its residue will yield the correct behaviour for (3.5). Once the solution has been obtained, by continuity it should remain valid as $\epsilon \rightarrow 0$.

In what follows, in particular when drawing explanatory diagrams, unless stated otherwise, we will assume that a_1 and a_2 are both negative. We will make sure to provide accurate ways of dealing with the case $a_{1,2} > 0$ when necessary.

3.4 Set notations

Let us start by introducing notations to describe useful sets in the α_1 and α_2 planes. We define the lower-half planes LHP_1 and LHP_2 and upper-half planes UHP_1 and UHP_2 as follows:

$$\begin{aligned} \text{LHP}_1 &= \{\alpha_1 \in \mathbb{C}, \text{ s.t. } \alpha_1 \text{ lies below } \mathcal{A}_1\}, \quad \text{LHP}_2 = \{\alpha_2 \in \mathbb{C}, \text{ s.t. } \alpha_2 \text{ lies below } \mathcal{A}_2\}, \\ \text{UHP}_1 &= \{\alpha_1 \in \mathbb{C}, \text{ s.t. } \alpha_1 \text{ lies above } \mathcal{A}_1\}, \quad \text{UHP}_2 = \{\alpha_2 \in \mathbb{C}, \text{ s.t. } \alpha_2 \text{ lies above } \mathcal{A}_2\}. \end{aligned}$$

³Note that this particular aspect is studied more rigorously in [9].

Note that these sets are defined to be inclusive of the contour \mathcal{A}_1 and \mathcal{A}_2 in the sense that $\mathcal{A}_1 = \text{LHP}_1 \cap \text{UHP}_1$ and $\mathcal{A}_2 = \text{LHP}_2 \cap \text{UHP}_2$. The four types of sets introduced so far are illustrated in Figure 6.

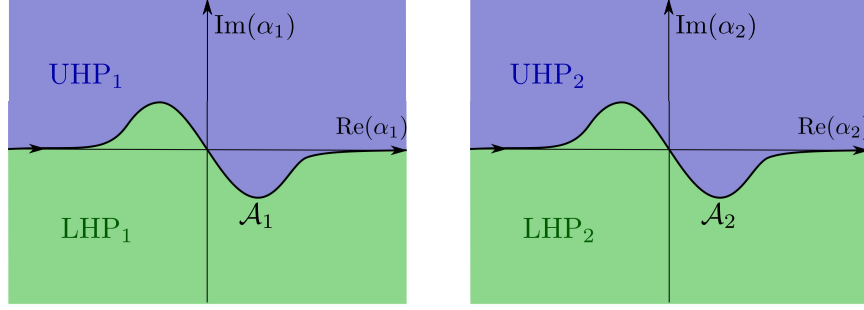


Figure 6: Diagrammatic description of the lower and upper-half planes used throughout this study.

Let us now define a few different \mathbb{C}^2 sets derived from various products of the \mathbb{C} spaces described above. We start with the set $\mathcal{D} = \mathcal{A}_1 \times \mathcal{A}_2$ where all of the functions we will deal with are well-behaved. It is also useful to define the \mathbb{C}^2 sets $\mathcal{D}_{++} = \text{UHP}_1 \times \text{UHP}_2$, $\mathcal{D}_{-+} = \text{LHP}_1 \times \text{UHP}_2$, $\mathcal{D}_{--} = \text{LHP}_1 \times \text{LHP}_2$ and $\mathcal{D}_{+-} = \text{UHP}_1 \times \text{LHP}_2$. Finally, let us introduce the sets $\mathcal{D}_{+\circ} = \mathcal{D}_{++} \cap \mathcal{D}_{+-} = \text{UHP}_1 \times \mathcal{A}_2$ and $\mathcal{D}_{-\circ} = \mathcal{D}_{--} \cap \mathcal{D}_{-+} = \text{LHP}_1 \times \mathcal{A}_2$.

With the above points regarding analyticity now clarified, we can return to $F(\alpha)$ given in (3.13) at the beginning of this subsection. It is clear that F is analytic on \mathcal{D}_{++} and hence we can rewrite it as

$$F(\alpha_1, \alpha_2) = 2iF_{++}(\alpha_1, \alpha_2). \quad (3.14)$$

4 On the four-part factorisation of K

Let us consider again the function $K(\alpha)$ defined by (3.2). We have shown in Section 3.3.1 that $K(\alpha)$ is analytic on the product of contours $\mathcal{D} = \mathcal{A}_1 \times \mathcal{A}_2$. In this section, our aim is to show that there exist four functions $K_{++}(\alpha)$, $K_{+-}(\alpha)$, $K_{-+}(\alpha)$ and $K_{--}(\alpha)$, analytic on \mathcal{D}_{++} , \mathcal{D}_{+-} , \mathcal{D}_{-+} and \mathcal{D}_{--} respectively, such that for $\alpha \in \mathcal{D}$, we have

$$K(\alpha) = K_{++}(\alpha)K_{+-}(\alpha)K_{-+}(\alpha)K_{--}(\alpha).$$

4.1 Factorisation in the α_1 -plane

Because of the definitions (3.1) and (3.2) of κ and K , we have:

$$K(\alpha) = 1/\kappa(\kappa(k, \alpha_2), \alpha_1) = 1/\left(\sqrt[4]{\kappa(k, \alpha_2) - \alpha_1}\sqrt[4]{\kappa(k, \alpha_2) + \alpha_1}\right), \quad (4.1)$$

and one can see that for any $\alpha \in \mathcal{D}$, it is possible to write

$$K(\alpha) = K_{-\circ}(\alpha)K_{+\circ}(\alpha),$$

such that for a given $\alpha_2 \in \mathcal{A}_2$, $K_{-\circ}(\alpha_1, \alpha_2)$ is analytic (as a function of α_1) in LHP_1 and $K_{+\circ}(\alpha_1, \alpha_2)$ is analytic (as a function of α_1) in UHP_1 . Exact expressions for $K_{-\circ}$ and $K_{+\circ}$ follow from (4.1):

$$K_{-\circ}(\alpha) = 1/\sqrt[4]{\kappa(k, \alpha_2) - \alpha_1} \text{ and } K_{+\circ}(\alpha) = 1/\sqrt[4]{\kappa(k, \alpha_2) + \alpha_1}. \quad (4.2)$$

Indeed, for a given $\alpha_2 \in \mathcal{A}_2$, the only branch point of $K_{-\circ}(\alpha)$ is at $\alpha_1 = \kappa(k, \alpha_2)$, which is strictly within UHP_1 so that $K_{-\circ}(\alpha)$ is a *minus function* when considered as a function of α_1 , i.e., it is analytic in LHP_1 . Similarly, the only branch point of $K_{+\circ}(\alpha)$ is at $\alpha_1 = -\kappa(k, \alpha_2)$, which is strictly within LHP_1 so that $K_{+\circ}(\alpha)$ is a *plus function* when considered as a function of α_1 , i.e. it is analytic in UHP_1 . This factorisation is illustrated in Figure 7.

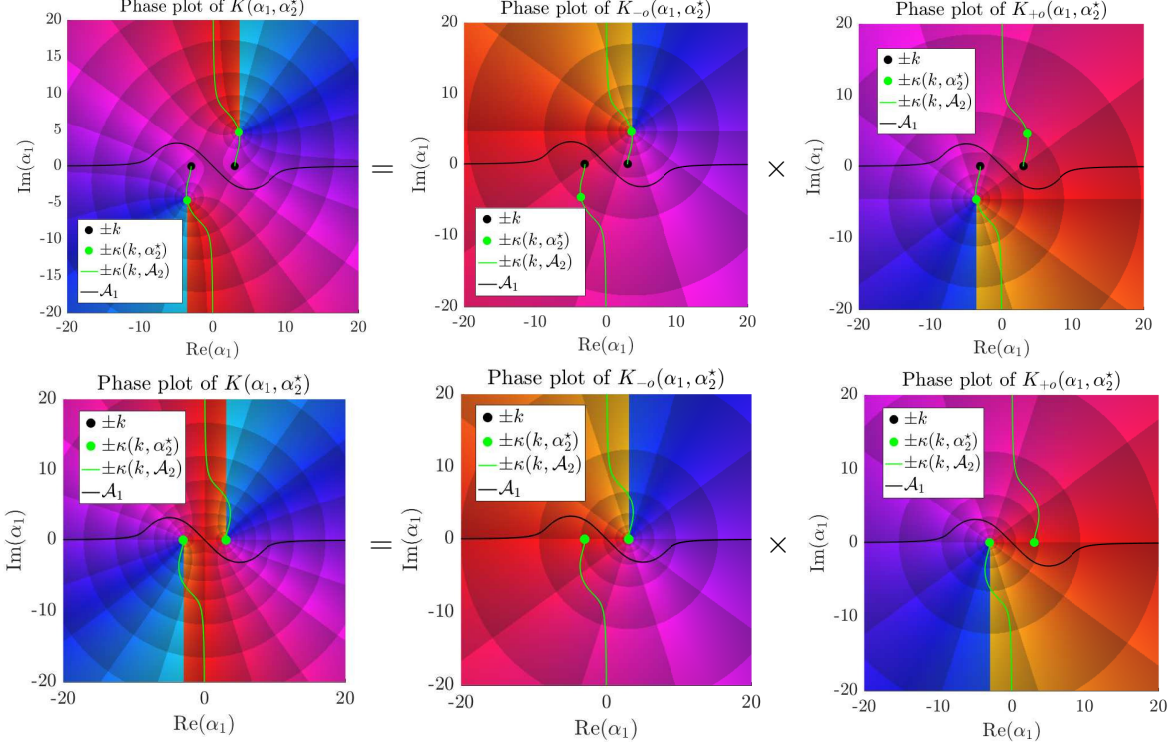


Figure 7: Plots of the functions $K(\alpha_1, \alpha_2^*)$, $K_{-\circ}(\alpha_1, \alpha_2^*)$ and $K_{+\circ}(\alpha_1, \alpha_2^*)$ in the α_1 complex plane for $\alpha_2^* = \mathcal{A}_2(5)$ (top) and $\alpha_2^* = \mathcal{A}_2(0)$ (bottom).

It must be stressed that these functions do not have any useful analyticity properties when viewed as functions of α_2 , with branch cuts passing through both UHP_2 and LHP_2 as α_1 moves along \mathcal{A}_1 . This can be seen in Figure 8.

It is also possible to introduce the functions $K_{\circ-}$ and $K_{\circ+}$ defined as follows:

$$K_{\circ-}(\alpha_1, \alpha_2) = 1/\sqrt[4]{\kappa(k, \alpha_1) - \alpha_2} \text{ and } K_{\circ+}(\alpha_1, \alpha_2) = 1/\sqrt[4]{\kappa(k, \alpha_1) + \alpha_2}, \quad (4.3)$$

which will prove useful in Section 4.2.2.

4.2 Factorisation in the α_2 -plane

4.2.1 Cauchy's formula and its application to factorisation problems

Let us state two useful results in complex analysis, that we will need in this section. The results are classic, and hence, the proofs are omitted. Please refer to e.g. [25] for more details. Note that these are valid for a generic complex plane, and since in what we have done so far \mathcal{A}_1 and \mathcal{A}_2 are the same, we will just denote it by \mathcal{A} in what follows. Similarly, we will use UHP and LHP without subscript.

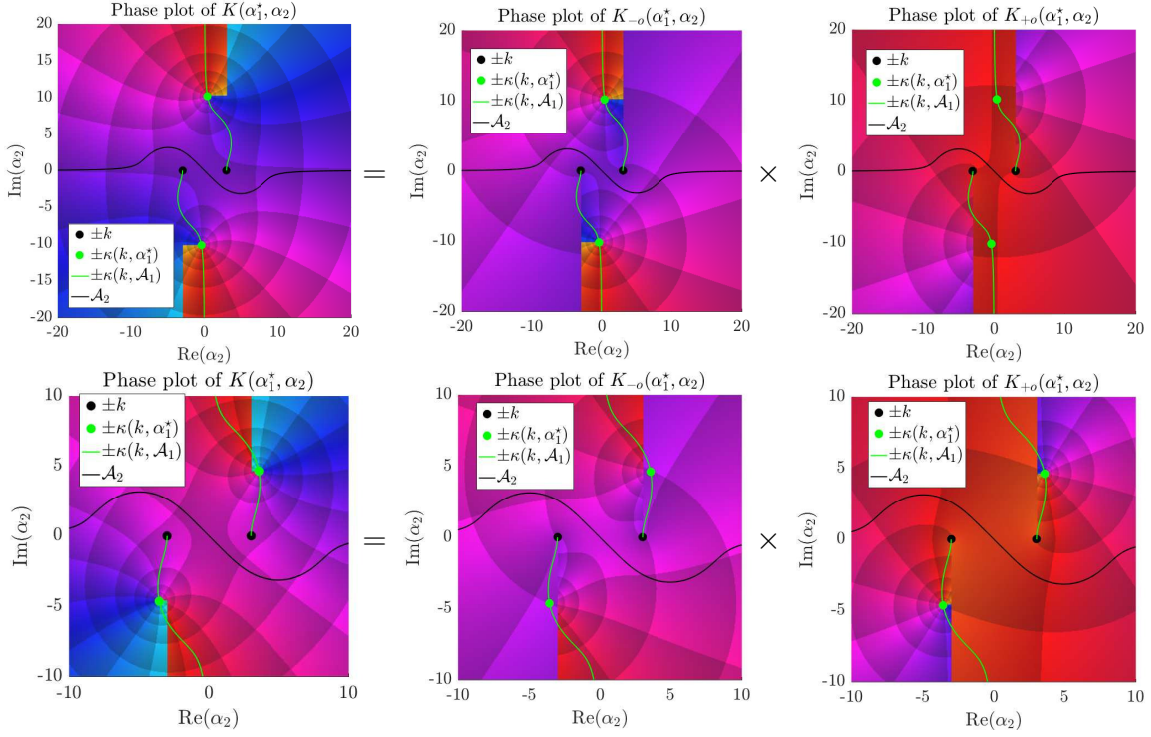


Figure 8: Plots of the functions $K(\alpha_1^*, \alpha_2)$, $K_{-o}(\alpha_1^*, \alpha_2)$ and $K_{+o}(\alpha_1^*, \alpha_2)$ in the α_2 complex plane for $\alpha_1^* = \mathcal{A}_1(10)$ (top) and $\alpha_1^* = \mathcal{A}_1(5)$ (bottom).

Lemma 4.1 [Cauchy's formula and sum-split] *Let Φ be a function analytic on a (potentially curved) strip $\mathcal{S} \subset \mathbb{C}$ containing \mathcal{A} , such that we have $\Phi(\alpha) = \Phi_+(\alpha) + \Phi_-(\alpha)$ on \mathcal{A} with Φ_+ analytic on UHP and Φ_- analytic on LHP. Consider $\mathcal{A}_\varepsilon^b$ and $\mathcal{A}_\varepsilon^a$ to be the contours oriented from left to right defined by $\mathcal{A}_\varepsilon^b = \mathcal{A} - i\varepsilon$ and $\mathcal{A}_\varepsilon^a = \mathcal{A} + i\varepsilon$, where $\varepsilon > 0$ is any number such that these contours lie within \mathcal{S} and the superscripts a and b stand for “above” and “below” respectively, as illustrated in Figure 9. Let $\alpha \in \mathcal{A}$, then, provided that $\Phi(z) = \mathcal{O}(1/|z|^\lambda)$ for some $\lambda > 0$ as $|z| \rightarrow \infty$ within \mathcal{S} , the following formulae hold*

$$\Phi_+(\alpha) = \frac{1}{2i\pi} \int_{\mathcal{A}_\varepsilon^b} \frac{\Phi(z)}{z - \alpha} dz \quad \text{and} \quad \Phi_-(\alpha) = \frac{-1}{2i\pi} \int_{\mathcal{A}_\varepsilon^a} \frac{\Phi(z)}{z - \alpha} dz,$$

and can be used to analytically continue Φ_+ (Φ_-) from \mathcal{A} onto UHP (LHP).

Corollary 4.1 [Cauchy's formula and factorisation] *Let Ψ be a function analytic on a (potentially curved) strip $\mathcal{S} \subset \mathbb{C}$ containing \mathcal{A} , such that we have $\Psi(\alpha) = \Psi_+(\alpha)\Psi_-(\alpha)$ on \mathcal{A} with Ψ_+ analytic on UHP and Ψ_- analytic on LHP. Let $\alpha \in \mathcal{A}$, then, provided that $\Psi(z) \rightarrow 1$ as $|z| \rightarrow \infty$ within \mathcal{S} , the following formulae hold*

$$\Psi_+(\alpha) = \exp \left\{ \frac{1}{2i\pi} \int_{\mathcal{A}_\varepsilon^b} \frac{\log(\Psi(z))}{z - \alpha} dz \right\} \quad \text{and} \quad \Psi_-(\alpha) = \exp \left\{ \frac{-1}{2i\pi} \int_{\mathcal{A}_\varepsilon^a} \frac{\log(\Psi(z))}{z - \alpha} dz \right\},$$

where $\mathcal{A}_\varepsilon^{a,b}$ are defined as in Lemma 4.1, and can be used to analytically continue Ψ_+ from \mathcal{A} onto UHP and Ψ_- from \mathcal{A} onto LHP.

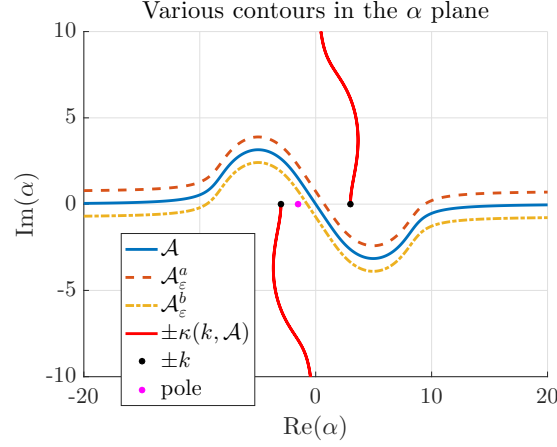


Figure 9: Diagrammatic illustrations of the contours introduced in Lemma 4.1

4.2.2 Factorisation of $K_{-\circ}$ and $K_{+\circ}$

It does not seem possible to find an *explicit* factorisation of these functions. Nevertheless, a direct application of Cauchy's formulae does lead to a formal factorisation of $K_{-\circ}$ and $K_{+\circ}$ in the α_2 plane. However, the resulting expressions can be quite slow to evaluate numerically. In Appendix A, we perform some manipulations of the integrals in order to obtain forms that are rapid to compute; these are employed in (4.4)-(4.7). $K_{-\circ}$ can be factorised as $K_{-\circ}(\alpha) = K_{-+}(\alpha)K_{--}(\alpha)$, and $K_{+\circ}$ can be factorised as $K_{+\circ}(\alpha) = K_{++}(\alpha)K_{+-}(\alpha)$, where we have

$$K_{-+}(\alpha) = \frac{1}{\sqrt[3]{\sqrt[3]{k} + \alpha_2}} \exp \left\{ \frac{-1}{4i\pi} \int_{\mathcal{A}_\varepsilon^b} \frac{\check{\log} \left(1 - \frac{\alpha_1}{\kappa(k,z)} \right)}{z - \alpha_2} dz \right\} \text{ for } \alpha \in \mathcal{D}_{-+}, \quad (4.4)$$

$$K_{--}(\alpha) = \frac{1}{\sqrt[3]{\sqrt[3]{k} - \alpha_2}} \exp \left\{ \frac{1}{4i\pi} \int_{\mathcal{A}_\varepsilon^a} \frac{\check{\log} \left(1 - \frac{\alpha_1}{\kappa(k,z)} \right)}{z - \alpha_2} dz \right\} \text{ for } \alpha \in \mathcal{D}_{--}, \quad (4.5)$$

$$K_{++}(\alpha) = \frac{1}{\sqrt[3]{\sqrt[3]{k} + \alpha_2}} \exp \left\{ \frac{-1}{4i\pi} \int_{\mathcal{A}_\varepsilon^b} \frac{\check{\log} \left(1 + \frac{\alpha_1}{\kappa(k,z)} \right)}{z - \alpha_2} dz \right\} \text{ for } \alpha \in \mathcal{D}_{++}, \quad (4.6)$$

$$K_{+-}(\alpha) = \frac{1}{\sqrt[3]{\sqrt[3]{k} - \alpha_2}} \exp \left\{ \frac{1}{4i\pi} \int_{\mathcal{A}_\varepsilon^a} \frac{\check{\log} \left(1 + \frac{\alpha_1}{\kappa(k,z)} \right)}{z - \alpha_2} dz \right\} \text{ for } \alpha \in \mathcal{D}_{+-}. \quad (4.7)$$

These formulae allow for a fast evaluation of the four components of the factorisation of K , allowing us to gain a good *visual* understanding of the singularity structure of K_{-+} , K_{--} , K_{++} and K_{+-} , as illustrated in Figures 10 and 11. To give an idea of the speed, for each plot we need to evaluate the functions 160,000 times and it takes about 14 seconds to run on a standard laptop.

Another method (see e.g. [4]), involving the Dilog function, has also been used to evaluate these factors. Both methods are very fast to evaluate, though, upon implementing them both in Matlab, it transpires that ours leads to a faster evaluation of K_{++} say. Moreover, our formula (4.6) giving K_{++} is more compact than that involving the Dilog function.

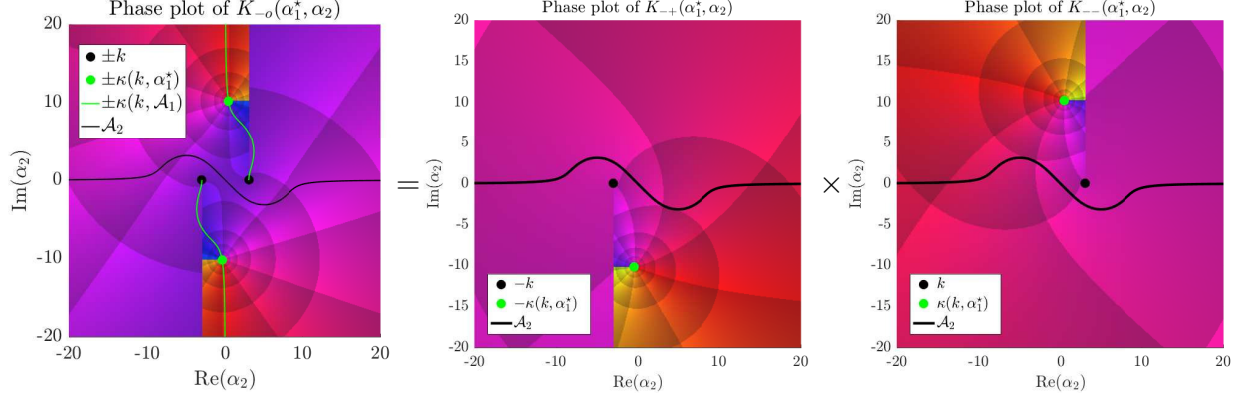


Figure 10: Plots of the functions $K_{-o}(\alpha_1^*, \alpha_2)$, $K_{-+}(\alpha_1^*, \alpha_2)$ and $K_{--}(\alpha_1^*, \alpha_2)$ in the α_2 complex plane for $\alpha_1^* = \mathcal{A}_1(10)$. In its region of analyticity, UHP₂, K_{-+} has been obtained via (4.4), while in LHP₂, it has been obtained by analytical continuation using $K_{-+} = K_{-o}/K_{--}$. A similar strategy has been used to plot K_{--} .

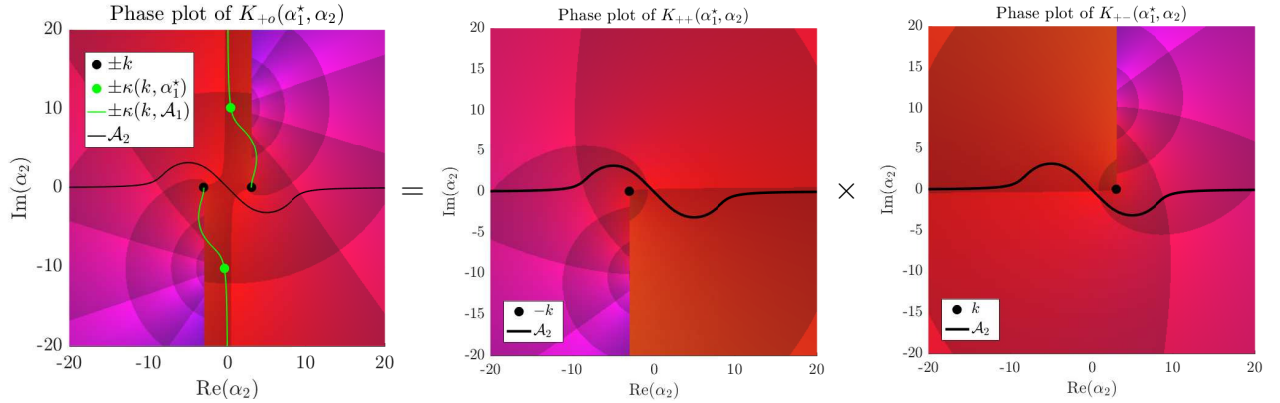


Figure 11: Plots of the functions $K_{+o}(\alpha_1^*, \alpha_2)$, $K_{++}(\alpha_1^*, \alpha_2)$ and $K_{+-}(\alpha_1^*, \alpha_2)$ in the α_2 complex plane for $\alpha_1^* = \mathcal{A}_1(10)$. In its region of analyticity, UHP₂, K_{++} has been obtained via (4.6), while in LHP₂, it has been obtained by analytical continuation using $K_{++} = K_{+o}/K_{+-}$. A similar strategy has been used to plot K_{+-} .

On Figures 10 and 11, α_1^* has been chosen on \mathcal{A}_1 for illustration purpose, but it could have been chosen anywhere in LHP_1 for Figure 10 and anywhere in UHP_1 for Figure 11. We chose to visualise this factorisation in the α_2 plane, but it is also possible to visualise it in the α_1 plane for a given α_2^* on \mathcal{A}_2 . In this case, in order to analytically continue the factors past their natural domain of analyticity, one should use the functions $K_{\circ\pm}$ introduced in (4.3).

5 The (generic) Wiener-Hopf system in \mathbb{C}^2

5.1 Quadruple sum-split

Using the function F_{++} defined in (3.14), the functional equation (3.10) can be rewritten $G(\alpha) = F_{++}(\alpha)K(\alpha)$ and, as seen in Section 3, G is analytic on $\mathcal{D} = \mathcal{A}_1 \times \mathcal{A}_2$. Hence, we can⁴ write its additive decomposition

$$F_{++}(\alpha)K(\alpha) = G(\alpha) = G_{++}(\alpha) + G_{-+}(\alpha) + G_{--}(\alpha) + G_{+-}(\alpha), \quad (5.1)$$

where $G_{++}(\alpha)$, $G_{-+}(\alpha)$, $G_{--}(\alpha)$ and $G_{+-}(\alpha)$ are analytic on \mathcal{D}_{++} , \mathcal{D}_{-+} , \mathcal{D}_{--} and \mathcal{D}_{+-} respectively. Note that by definition of $G(\alpha)$, see (3.5), we have $G(\alpha) = \mathfrak{F}[u(x_1, x_2, 0)](\alpha)$, where \mathfrak{F} is the double Fourier transform operator as defined in Section 3.2. Therefore, upon defining the functions u_j , $j = 1 \dots 4$, by

$$u_j(x_1, x_2) = u(x_1, x_2, 0)H_j(x_1, x_2), \text{ where } H_j(x_1, x_2) = \begin{cases} 1 & \text{if } (x_1, x_2) \in \mathcal{Q}_j, \\ 0 & \text{otherwise,} \end{cases}$$

it is then possible to define the additive terms as quarter-range Fourier transforms:

$$\begin{aligned} G_{++}(\alpha) &= \mathfrak{F}[u_1(x_1, x_2)](\alpha), \quad G_{-+}(\alpha) = \mathfrak{F}[u_2(x_1, x_2)](\alpha), \\ G_{--}(\alpha) &= \mathfrak{F}[u_3(x_1, x_2)](\alpha), \quad G_{+-}(\alpha) = \mathfrak{F}[u_4(x_1, x_2)](\alpha). \end{aligned} \quad (5.2)$$

We can also define the auxiliary functions $G_{+\circ} = G_{++} + G_{+-}$ and $G_{-\circ} = G_{-+} + G_{--}$ that are analytic on $\mathcal{D}_{+\circ}$ and $\mathcal{D}_{-\circ}$ respectively.

5.2 On the function G_{++}

Because we impose the Dirichlet condition (2.4), it follows that we have

$$u_1(x_1, x_2) = -u_{\text{in}}(x_1, x_2, 0)H_1(x_1, x_2) = -e^{-i(a_1x_1 + a_2x_2)}H_1(x_1, x_2)$$

and so, since G_{++} is defined on \mathcal{D}_{++} by $G_{++}(\alpha) = \mathfrak{F}[u_1(x_1, x_2)](\alpha)$, we obtain

$$G_{++}(\alpha) = \frac{1}{(\alpha_1 - a_1)(\alpha_2 - a_2)}. \quad (5.3)$$

Note that each pole must lie in its respective lower-half plane whether $a_{1,2}$ is positive or negative in order to ensure that G_{++} is analytic in \mathcal{D}_{++} . As discussed in Remark 3.1, when $a_{1,2}$ is positive, we allow it to have a small imaginary part, $\epsilon < 0$, which places it below $\mathcal{A}_{1,2}$, and then later allow $\epsilon \rightarrow 0$.

Hence, at the moment, we have four unknown functions, namely F_{++} , G_{+-} , G_{-+} and G_{--} . In the following two subsections, we will show how (5.1) can be reduced to four equations, involving our four unknowns.

⁴A more rigorous approach to obtain this would be to refer to Bochner's theorem [14].

5.3 A first split, in the α_1 plane

Let us start by rewriting⁵ (5.1) as follows:

$$F_{++}K_{+o}K_{-o} = G_{++} + G_{-o} + G_{+-}.$$

Upon dividing by K_{-o} , we obtain

$$F_{++}K_{+o} = G_{++}/K_{-o} + G_{-o}/K_{-o} + G_{+-}/K_{-o}. \quad (5.4)$$

Now, formally, using for example Lemma 4.1, it is possible to perform a sum-split in the α_1 -plane of the terms G_{++}/K_{-o} and G_{+-}/K_{-o} by writing

$$\frac{G_{++}}{K_{-o}} = \left[\frac{G_{++}}{K_{-o}} \right]_{+o} + \left[\frac{G_{++}}{K_{-o}} \right]_{-o} \text{ and } \frac{G_{+-}}{K_{-o}} = \left[\frac{G_{+-}}{K_{-o}} \right]_{+o} + \left[\frac{G_{+-}}{K_{-o}} \right]_{-o},$$

where the operators $[]_{-o}$ and $[]_{+o}$ represent respectively the α_1 -minus part and α_1 -plus part of a given function that is analytic on \mathcal{A}_1 when considered a function of α_1 . With this split, (5.4) may be rearranged as

$$F_{++}K_{+o} - \left[\frac{G_{++}}{K_{-o}} \right]_{+o} - \left[\frac{G_{+-}}{K_{-o}} \right]_{+o} = \frac{G_{-o}}{K_{-o}} + \left[\frac{G_{++}}{K_{-o}} \right]_{-o} + \left[\frac{G_{+-}}{K_{-o}} \right]_{-o}. \quad (5.5)$$

Because of the simplicity of G_{++} (see (5.3)), the sum-split of G_{++}/K_{-o} can be achieved explicitly via the pole removal technique:

$$\left[\frac{G_{++}}{K_{-o}} \right]_{+o} = \frac{G_{++}}{K_{-o}(a_1, \alpha_2)} \text{ and } \left[\frac{G_{++}}{K_{-o}} \right]_{-o} = G_{++} \left(\frac{1}{K_{-o}} - \frac{1}{K_{-o}(a_1, \alpha_2)} \right).$$

Now, by construction, the left-hand side (LHS) of (5.5) is analytic in \mathcal{D}_{+o} , while the right-hand side (RHS) of (5.5) is analytic in \mathcal{D}_{-o} . Hence it is possible to use (5.5) to construct a function E_{1o} that is analytic on $\mathbb{C} \times \mathcal{A}_2$ and defined by

$$E_{1o} = \begin{cases} F_{++}K_{+o} - \frac{G_{++}}{K_{-o}(a_1, \alpha_2)} - \left[\frac{G_{+-}}{K_{-o}} \right]_{+o} & \text{if } \alpha \in \mathcal{D}_{+o}, \\ \frac{G_{-o}}{K_{-o}} + G_{++} \left(\frac{1}{K_{-o}} - \frac{1}{K_{-o}(a_1, \alpha_2)} \right) + \left[\frac{G_{+-}}{K_{-o}} \right]_{-o} & \text{if } \alpha \in \mathcal{D}_{-o}. \end{cases} \quad (5.6)$$

Moreover, it can be shown that it tends to zero as $|\alpha_1| \rightarrow \infty$ (see Appendix B.2), and so we can apply Liouville's theorem in the α_1 plane to get $E_{1o} \equiv 0$; hence

$$F_{++}K_{+o} - \frac{G_{++}}{K_{-o}(a_1, \alpha_2)} - \left[\frac{G_{+-}}{K_{-o}} \right]_{+o} = 0, \quad (5.7)$$

$$\frac{G_{-o}}{K_{-o}} + G_{++} \left(\frac{1}{K_{-o}} - \frac{1}{K_{-o}(a_1, \alpha_2)} \right) + \left[\frac{G_{+-}}{K_{-o}} \right]_{-o} = 0. \quad (5.8)$$

⁵For brevity we will only specify the argument of the functions involved if it is not α .

5.4 A second split, in the α_2 plane

Upon multiplying equation (5.7) by $K_{-+}(a_1, \alpha_2)/K_{+-}$, it becomes

$$F_{++}K_{++}K_{-+}(a_1, \alpha_2) = \frac{G_{++}}{K_{--}(a_1, \alpha_2)K_{+-}} + \frac{K_{-+}(a_1, \alpha_2)}{K_{+-}} \left[\frac{G_{+-}}{K_{-\circ}} \right]_{+\circ}. \quad (5.9)$$

The LHS is a $++$ function, and, once again, formally, using Lemma 4.1, each of the two terms on the RHS of (5.9) has a sum-split decomposition in the α_2 plane (the associated operators being denoted $[\]_{\circ-}$ and $[\]_{\circ+}$), such that we can rewrite (5.9) as

$$\begin{aligned} F_{++}K_{++}K_{-+}(a_1, \alpha_2) - \left[\frac{G_{++}}{K_{--}(a_1, \alpha_2)K_{+-}} \right]_{\circ+} - \left[\frac{K_{-+}(a_1, \alpha_2)}{K_{+-}} \left[\frac{G_{+-}}{K_{-\circ}} \right]_{+\circ} \right]_{\circ+} \\ = \left[\frac{G_{++}}{K_{--}(a_1, \alpha_2)K_{+-}} \right]_{\circ-} + \left[\frac{K_{-+}(a_1, \alpha_2)}{K_{+-}} \left[\frac{G_{+-}}{K_{-\circ}} \right]_{+\circ} \right]_{\circ-}. \end{aligned} \quad (5.10)$$

Again, because of the form of G_{++} , the related split can be performed explicitly by pole removal to get

$$\begin{aligned} \left[\frac{G_{++}}{K_{--}(a_1, \alpha_2)K_{+-}} \right]_{\circ-} &= G_{++} \left(\frac{1}{K_{--}(a_1, \alpha_2)K_{+-}} - \frac{1}{K_{--}(a_1, a_2)K_{+-}(\alpha_1, a_2)} \right), \\ \left[\frac{G_{++}}{K_{--}(a_1, \alpha_2)K_{+-}} \right]_{\circ+} &= \frac{G_{++}}{K_{--}(a_1, a_2)K_{+-}(\alpha_1, a_2)}. \end{aligned}$$

Now, by inspection, it is clear that the LHS of (5.10) is analytic on \mathcal{D}_{++} , while its RHS is analytic on \mathcal{D}_{+-} . Hence, it is possible to construct a function E_{+2} that is analytic on $\text{UHP}_1 \times \mathbb{C}$ and defined by

$$E_{+2} = \begin{cases} F_{++}K_{++}K_{-+}(a_1, \alpha_2) - \frac{G_{++}}{K_{--}(a_1, a_2)K_{+-}(\alpha_1, a_2)} - \left[\frac{K_{-+}(a_1, \alpha_2)}{K_{+-}} \left[\frac{G_{+-}}{K_{-\circ}} \right]_{+\circ} \right]_{\circ+} & \text{if } \alpha \in \mathcal{D}_{++}, \\ G_{++} \left(\frac{1}{K_{--}(a_1, \alpha_2)K_{+-}} - \frac{1}{K_{--}(a_1, a_2)K_{+-}(\alpha_1, a_2)} \right) + \left[\frac{K_{-+}(a_1, \alpha_2)}{K_{+-}} \left[\frac{G_{+-}}{K_{-\circ}} \right]_{+\circ} \right]_{\circ-} & \text{if } \alpha \in \mathcal{D}_{+-}. \end{cases} \quad (5.11)$$

One of the aims of this work is to provide a *constructive path* towards Radlow's ansatz. In order to do so, we wish to apply Liouville's theorem in the α_2 plane and, for this, we need to examine the right-hand sides of (5.11) as $|\alpha_2| \rightarrow \infty$ in their respective half-planes of analyticity. Using the proof given in Appendix B.3, we can show that $E_{+2} \equiv 0$ and hence obtain the two main equations of the paper:

$$F_{++} = \frac{G_{++}}{K_{++}K_{-+}(a_1, \alpha_2)K_{--}(a_1, a_2)K_{+-}(\alpha_1, a_2)} \quad (5.12)$$

$$\begin{aligned} &+ \frac{1}{K_{++}K_{-+}(a_1, \alpha_2)} \left[\frac{K_{-+}(a_1, \alpha_2)}{K_{+-}} \left[\frac{G_{+-}}{K_{-\circ}} \right]_{+\circ} \right]_{\circ+}, \\ 0 &= G_{++} \left(\frac{1}{K_{--}(a_1, \alpha_2)K_{+-}} - \frac{1}{K_{--}(a_1, a_2)K_{+-}(\alpha_1, a_2)} \right) \\ &+ \left[\frac{K_{-+}(a_1, \alpha_2)}{K_{+-}} \left[\frac{G_{+-}}{K_{-\circ}} \right]_{+\circ} \right]_{\circ-}. \end{aligned} \quad (5.13)$$

Remember that in order to recover the physical field everywhere via (3.11), the unknown of interest is the function $F_{++}(\alpha)$. We can at this stage make two important remarks regarding

(5.12). Firstly, provided that we know the function G_{+-} , then F_{++} can in theory be recovered. Secondly, it is important to note that the first term on the RHS of (5.12) is exactly Radlow's ansatz published in [27]. The main issue with Radlow's solution was that the resulting physical field did not behave as expected near the tip of the quarter-plane (Radlow's ansatz predicts a behaviour of $\mathcal{O}(r^{1/4})$, while the correct behaviour is $\mathcal{O}(r^{\nu_1-1/2})$, where ν_1 is related to the first eigenvalue of the Laplace-Beltrami operator). As such the benefit of this equation is dual. On the one hand, it is clear that (5.12) indicates the error in Radlow's analysis, since a term is missing from his ansatz. On the other hand, we provide here a constructive procedure showing how this ansatz is obtained, which can be enlightening in view of the fact that no derivation was provided in Radlow's original work. Indeed, it was the fact that Radlow merely stated a solution in [27], that has partially led to difficulties in establishing and quantifying the error to-date.

In addition, we also know that the correct physical behaviour of the solution should be enforced by the term involving G_{+-} . Equation (5.13), that we will refer to as a *compatibility equation*, is very interesting in that respect. Firstly, it does not appear in Radlow's work, nor in any subsequent work to our knowledge. Secondly, if it can somehow be inverted (which in practice is a very difficult thing to do), it provides a way to obtain G_{+-} . Even though it is not possible to do this exactly (as the authors believe is the case), it provides a way of testing any approximation to G_{+-} . Hence, we believe that the compatibility equation (5.13) is key to solving the problem at hand. We will not go through this route in this paper, but it will be the basis of a future article.

Before going further, note also that (5.8) has not been used so far. It is possible to employ it to obtain two more equations involving G_{--} , G_{+-} and G_{-+} , by introducing similarly a function E_{-2} entire in the α_2 complex plane (which is again zero by application of Liouville's theorem). However, we do not believe that these will provide further information on the solution, and so are extraneous. Moreover, nowhere in this section did we use the definition of $\mathcal{A}_{1,2}$ explicitly; hence the results obtained remain valid when a_1 or a_2 are positive.

To summarise, in order to solve our problem and find F_{++} , we need to gain some information about G_{+-} and find an approximation that will be compatible both with the physics of the problem and with the compatibility equation (5.13). A possible approximation scheme for G_{+-} , involving an explicit canonical integral, is suggested in [5]. However, for the purpose of this paper, let us assume that we know F_{++} and let us try to find out what can be inferred about the diffraction coefficient.

5.5 Link with diffraction coefficient

Classically, (see e.g. [6, 7]) the Dirichlet corner diffraction coefficient $f^d(\theta, \varphi, \theta_0, \varphi_0)$ is defined by

$$u_{\text{sph}} \underset{kr \rightarrow \infty}{\approx} 2\pi \frac{e^{ikr}}{kr} f^d(\theta, \varphi; \theta_0, \varphi_0), \quad (5.14)$$

where u_{sph} represents the spherical wave emanating from the tip. Assuming that F_{++} is known, using complexified spherical coordinates, one can apply a double steepest-descent analysis as $kr \rightarrow \infty$ [12, 2] to obtain the following relationship between the diffraction coefficient and F_{++} :

$$f^d(\theta, \varphi; \theta_0, \varphi_0) = \frac{kF_{++}(-k \cos(\varphi) \sin(\theta), -k \sin(\varphi) \sin(\theta))}{4\pi^2 i}. \quad (5.15)$$

We believe that this formula should remain valid everywhere. We may of course get other far-field contributions (edge-diffracted waves, reflected wave, etc.) that will result from crossing poles when deforming the various contours to their steepest-descent paths. However, the $1/kr$ component can

only be the one given in (5.15). In particular, it should have the same singular regions as those obtained (explicitly) with the embedding procedure, but most importantly, this formula should be valid in the regions that the embedding formulae cannot (yet) reach. We can easily observe that the polar singularity structure is similar. In fact we have seen in [6] that if we write $\xi = \cos(\varphi) \sin(\theta)$, $\xi_0 = \cos(\varphi_0) \sin(\theta_0)$, $\eta = \sin(\varphi) \sin(\theta)$ and $\eta_0 = \sin(\varphi_0) \sin(\theta_0)$, the diffraction coefficient had simple poles when $\xi = -\xi_0$ and $\eta = -\eta_0$. Upon noticing that in (5.15) we evaluate F_{++} at $(\alpha_1, \alpha_2) = (-k\xi, -k\eta)$, realising that $(a_1, a_2) = (k\xi_0, k\eta_0)$, and remembering that F_{++} has poles at $\alpha_{1,2} = a_{1,2}$, we recover the expected polar singularities.

Note⁶ that (5.15) implies that the diffraction coefficient does not depend on k . To see this, let $v(\mathbf{x})$ be the scattered field of the Dirichlet quarter-plane problem for $k = 1$. One can show directly that, for $k > 0$, the solution u of our problem summarised in Section 2.5 is given by $u(\mathbf{x}) = v(k\mathbf{x})$. Using the basic definition of the double Fourier transform, and the fact that $\frac{\partial u}{\partial x_3}(x_1, x_2, 0^+) = 0$ on $Q_2 \cup Q_3 \cup Q_4$, we can show that $ikF_{++}(k\boldsymbol{\alpha}) = \mathfrak{F}[\frac{\partial v}{\partial x_3}(x_1, x_2, 0^+)](\boldsymbol{\alpha})$, which is clearly independent of k .

Another interesting feature to be considered is that we know [6] that the diffraction coefficient should in fact be purely imaginary (at least where the MSF are valid). However, it is not obvious that the RHS of (5.15) is indeed purely imaginary.

One issue with the formula (5.15) is that the function F_{++} is evaluated on the real interval $(-k, k)$ in both complex planes. However, it is clear from the above analysis that the segment $(-k, 0)$ does not lie in UHP_1 or UHP_2 . Hence, we are forced to evaluate a $++$ function *outside* \mathcal{D}_{++} . This problem can be dealt with by means of analytically continuing F_{++} within that region.

6 Comparison between Radlow's ansatz and MSF

In this section, we compare the diffraction coefficient obtained by the MSF to that obtained by using Radlow's *erroneous* ansatz. The MSF is now an established method known to be correct within a certain domain of the observer space. The idea of comparing both methods is mainly due to serendipity. Whilst testing a method to evaluate the effect of G_{+-} on the diffraction coefficient, we once accidentally set $G_{+-} = 0$, which is equivalent to using Radlow's ansatz exactly. To our surprise, this led to a very good agreement with the MSF results, where these formulae were valid. We decided to explore the incidence space, and so far we could not find any incident angle leading to an obvious disagreement between the two methods. Here we present four distinct incidences (we keep $\theta_0 = \pi/4$, and choose four different φ_0), corresponding to different signs for $a_{1,2}$. The chosen incidences are summarised in Figure 12.

For each incidence, we pick 8 arcs surrounding the quarter-plane on which we evaluate the diffraction coefficient. That is we pick 8 values of φ between 0 and 2π , and for each value of φ , we evaluate the coefficient for $\theta \in [0, \pi/2]$. The results are presented in Figures 13–16, showing very good agreement between the two methods. When the diffraction coefficient does not have any singularities, as in Figures 13(e)(f)(g), 14(e)(f)(g), 15(a)(g)(h) and 16(b), it means that the only far-field component in the observation region is the spherical wave emanating from the tip, this is the so-called oasis zone. The diffraction coefficient becomes singular at the boundaries of existence of the edge-diffracted fields. Another important point to mention is the validity of this ansatz in the region where the MSF are not valid (see [6] for discussion) due to double diffraction of the field (Figures 15(c) and 16(a)(c)). Passing the limit of validity, we notice that the diffraction

⁶The authors are most grateful to the anonymous reviewer for this and many other suggestions, which have significantly improved the clarity and focus of the article.

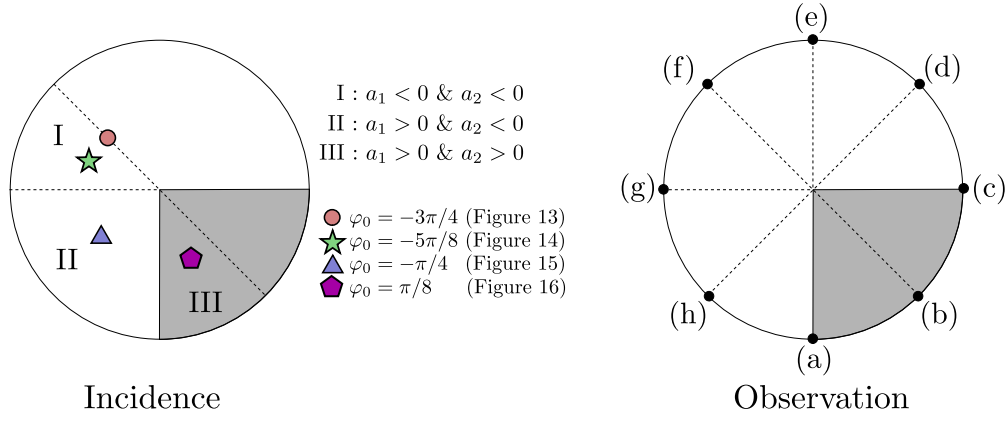


Figure 12: Left: Illustration of the incident angles used in the presentation of the results. We have ensured that each region corresponding to a different sign combination of a_1 and a_2 was considered. Right: Illustration of the 8 arcs of observation used in the presentation of the results.

coefficient given by Radlow's ansatz, which is purely imaginary everywhere else, becomes purely real. Mathematically this corresponds to saddle points going through a branch point during the steepest-descent procedure. Having no data to compare to in this region, it remains to be seen if this yields the correct physical solution.

The fact that Radlow's ansatz produces extremely accurate results for the diffraction coefficient is indeed surprising, but such possibility was not ruled out in Albani's work [3]. Indeed Albani's approach to showing that Radlow's ansatz (let us call it $F_{++}^{\text{Ra}}(\boldsymbol{\alpha})$) was incorrect was to demonstrate that the resulting physical field, $u^{\text{Ra}}(x_1, x_2, x_3)$ did not satisfy the boundary condition, i.e. was not equal to $-e^{-i(a_1 x_1 + a_2 x_2)}$ on the quarter-plane $x_{1,2} > 0$. An interesting point, however, was that he showed that as both x_1 and x_2 tend to infinity simultaneously, we have

$$u^{\text{Ra}}(x_1 > 0, x_2 > 0, 0) - (-e^{-i(a_1 x_1 + a_2 x_2)}) = \mathcal{O}((x_1^2 + x_2^2)^{-3/2}), \quad (6.1)$$

implying that in a way, the boundary conditions are *asymptotically satisfied* away from the vertex and the edges. The rapidity of the decay (one over the cube of the distance to the vertex) being much higher than the decay of the spherical wave (one over this distance) may be the beginning of an explanation as to why Radlow's ansatz performs so well in that case. It has to be said however that the agreement between the two methods cannot be perfect. Indeed, if it were to be, then F_{++} and F_{++}^{Ra} would have to be exactly the same on a non-isolated region, and hence, due to the theory of analytic functions, they will have to be the same everywhere, which as we showed would violate the compatibility condition. There must hence exist a numerical discrepancy between the two methods. In order to find it, we made sure that the MSF and the Radlow's ansatz were accurately evaluated up to a relative error of the order $\mathcal{O}(10^{-5})$ and looked at the pointwise difference between the two methods for the particular testcase of Figure 13(g). The results are displayed in Figure 17, and one can see that the relative error is of the order $\mathcal{O}(10^{-3})$, two orders of magnitude higher than the precision with which both methods were computed. We can hence conclude that this is an actual discrepancy between the two methods, and not a numerical artefact.

7 Conclusion

In this paper, we revisited Radlow's double Wiener-Hopf approach for the Dirichlet quarter-plane problem. We have tried to add more clarity and precision to his innovative approach, with an aim

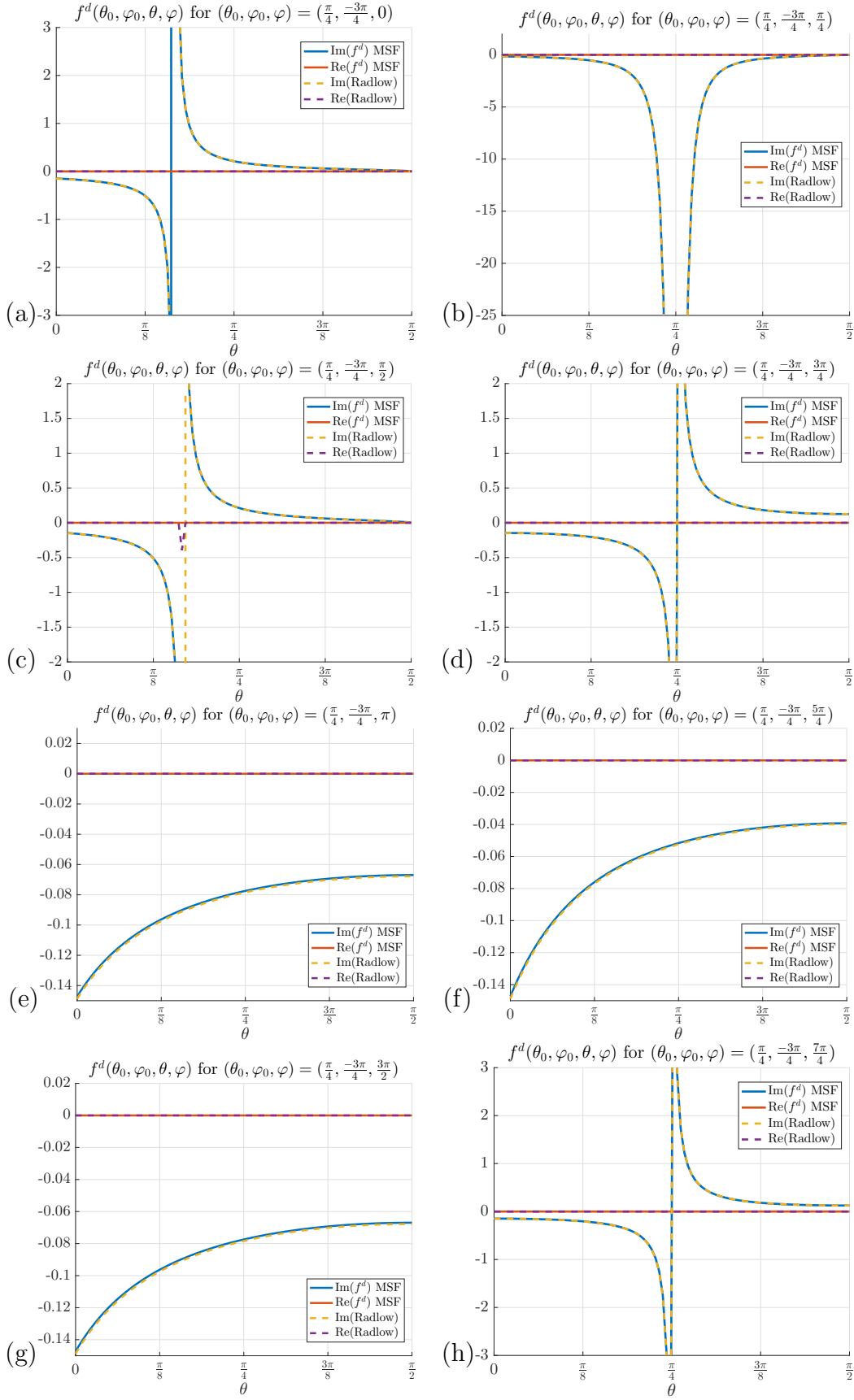


Figure 13: Diffraction coefficient for incidence $(\theta_0, \varphi_0) = (\pi/4, -3\pi/4)$, i.e. we have $a_1 < 0$ and $a_2 < 0$, with polar observation angle $\theta \in [0, \pi/2]$ and various values of the azimuthal observation angles $\varphi = 0, \pi/4, \pi/2, 3\pi/4, \pi, 5\pi/4, 3\pi/2, 7\pi/4$ (from (a) to (h)).

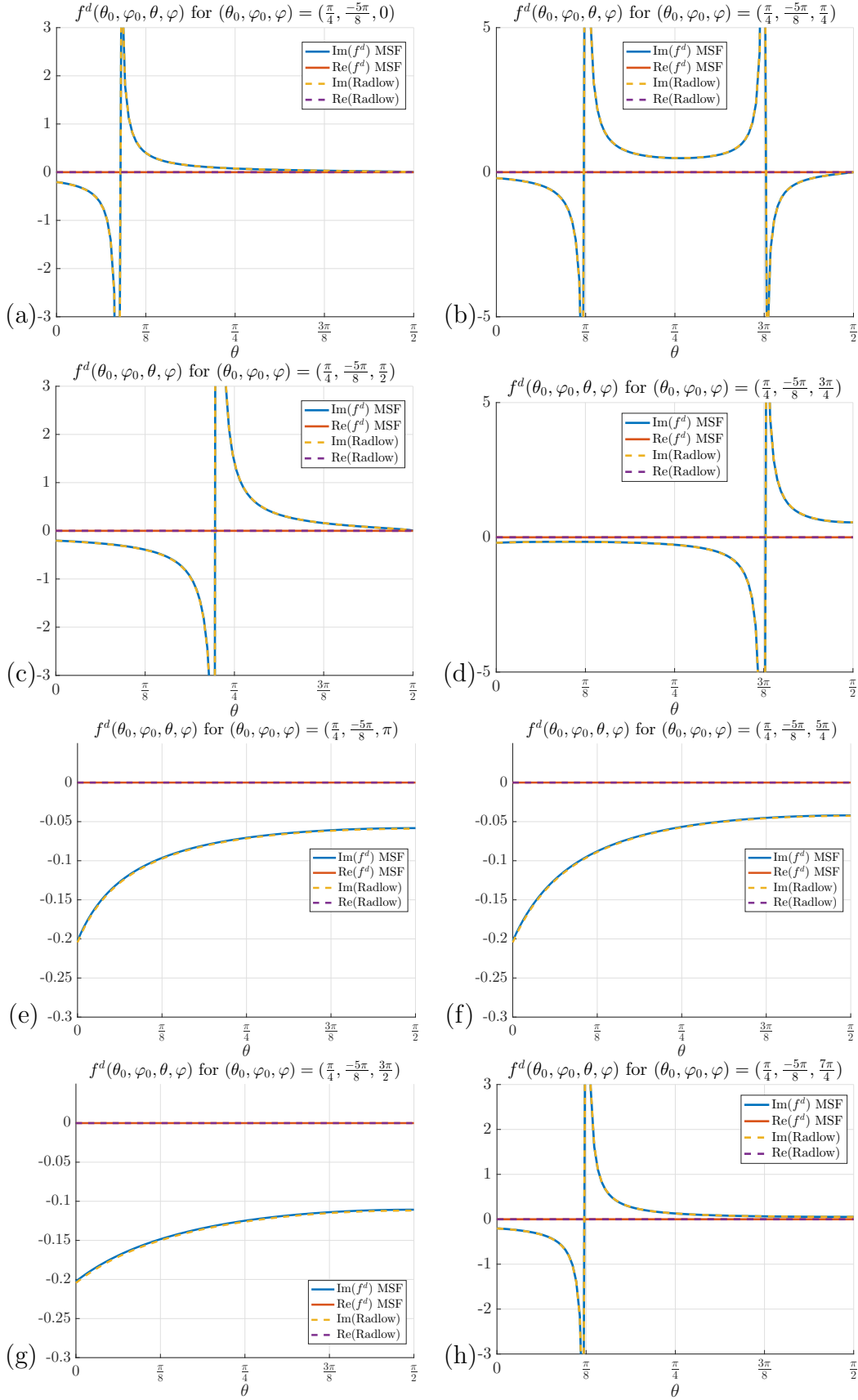


Figure 14: Diffraction coefficient for incidence $(\theta_0, \varphi_0) = (\frac{\pi}{4}, -\frac{5\pi}{8})$, i.e. we have $a_1 < 0$ and $a_2 < 0$, with polar observation angle $\theta \in [0, \frac{\pi}{2}]$ and various values of the azimuthal observation angles $\varphi = 0, \frac{\pi}{4}, \frac{\pi}{2}, \frac{3\pi}{4}, \pi, \frac{5\pi}{4}, \frac{3\pi}{2}, \frac{7\pi}{4}$ (from (a) to (h)).

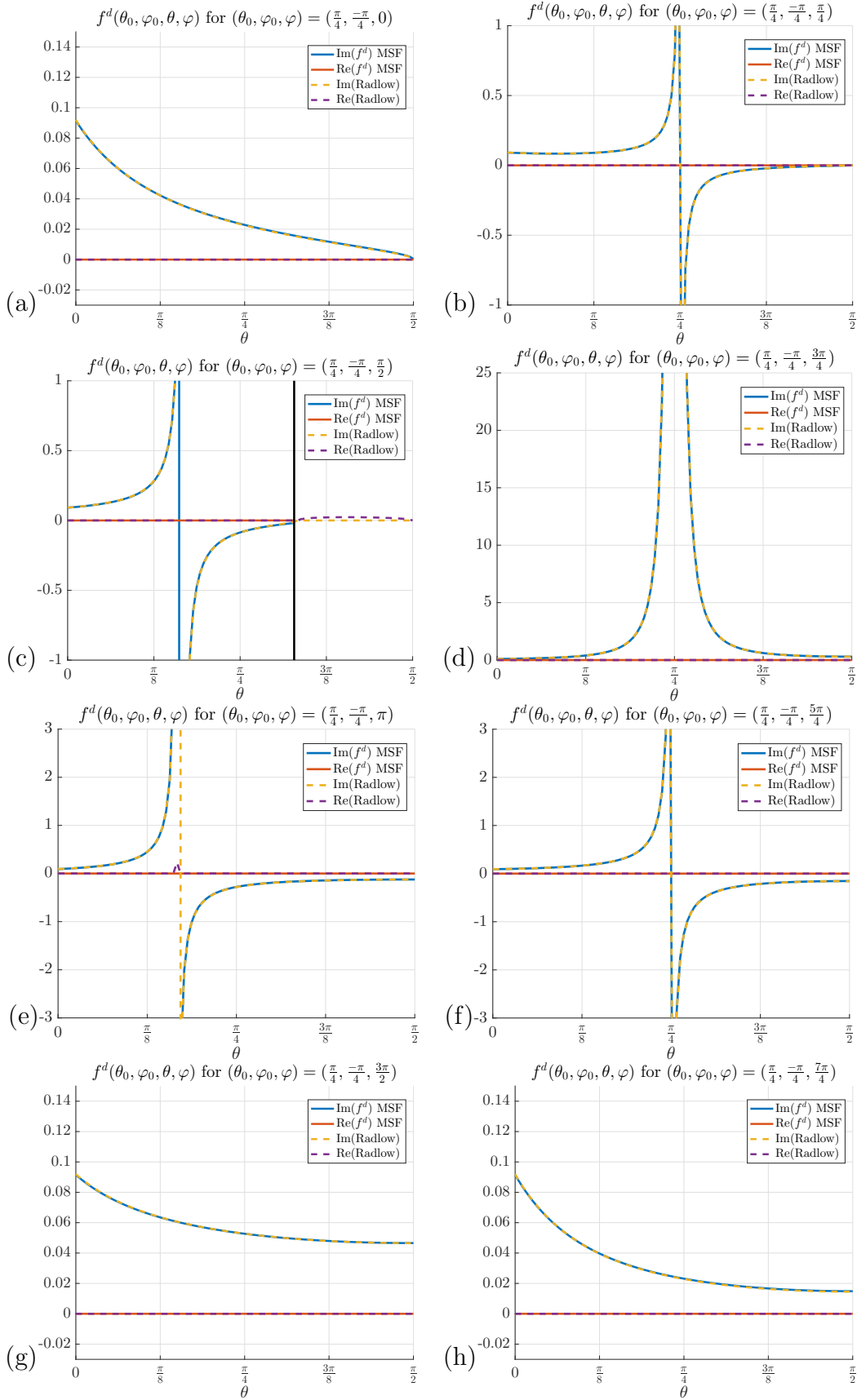


Figure 15: Diffraction coefficient for incidence $(\theta_0, \varphi_0) = (\frac{\pi}{4}, -\frac{\pi}{4})$, i.e. we have $a_1 > 0$ and $a_2 < 0$, with polar observation angle $\theta \in [0, \frac{\pi}{2}]$ and various values of the azimuthal observation angles $\varphi = 0, \frac{\pi}{4}, \frac{\pi}{2}, \frac{3\pi}{4}, \pi, \frac{5\pi}{4}, \frac{3\pi}{2}, \frac{7\pi}{4}$ (from (a) to (h)). In (c), the black vertical line represents the limit of validity of the MSF.

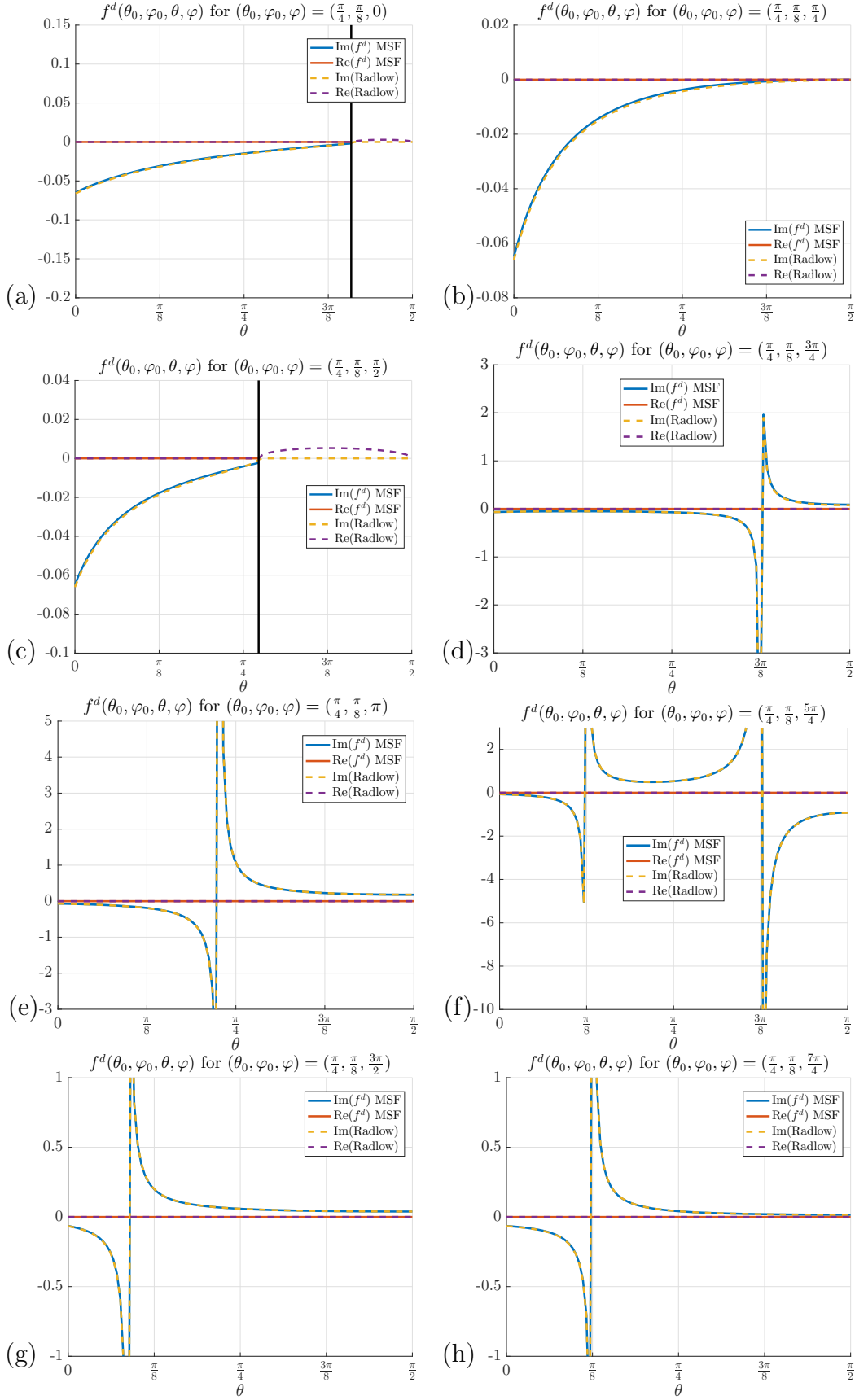


Figure 16: Diffraction coefficient for incidence $(\theta_0, \varphi_0) = (\frac{\pi}{4}, \frac{\pi}{8})$, i.e. we have $a_1 > 0$ and $a_2 > 0$, with polar observation angle $\theta \in [0, \frac{\pi}{2}]$ and various values of the azimuthal observation angles $\varphi = 0, \frac{\pi}{4}, \frac{\pi}{2}, \frac{3\pi}{4}, \pi, \frac{5\pi}{4}, \frac{3\pi}{2}, \frac{7\pi}{4}$ (from (a) to (h)). In (a) and (c), the vertical black line represents the limit of validity of the MSF.

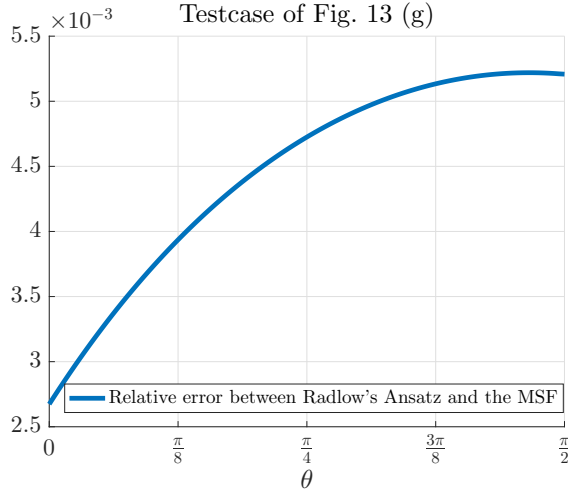


Figure 17: Pointwise relative error between the diffraction coefficient obtained by the MSF and by Radlow's ansatz for the testcase of Figure 13 (g).

to obtain a *constructive* method of solution of this canonical boundary value problem. The inverse Fourier transform (3.11), gives the solution in terms of an unknown function F_{++} , that depends on two complex variables. We reduced the problem to two equations, one, (5.12), expresses F_{++} as the sum of two terms, one containing the unknown function G_{+-} and the other being Radlow's ansatz. This, on the one hand, gives a constructive way of obtaining the ansatz, and on the other hand, offers yet another reason why this ansatz cannot be the true solution. The second equation, (5.13), called the *compatibility equation*, involves solely the unknown function G_{+-} and could be key to determining this crucial unknown function.

Finally, following a steepest-descent analysis, we have related F_{++} to the diffraction coefficient f^d . Numerical results show that when choosing F_{++} as per Radlow's ansatz, we obtain surprisingly accurate results for the diffraction coefficient. In fact, the results seem to agree very well with those obtained by the established Modified Smyshlyaev Formulae, where this method is valid. Theoretically, it is however impossible for this agreement to be perfect, and we have shown that there exists a small discrepancy between the two methods, with a relative error of order $\mathcal{O}(10^{-3})$. It should be noted that the MSF is a very quick way of evaluating the diffraction coefficient; however, Radlow's ansatz, and the factorisation formulae provided herein, is even faster (computing the Radlow result for each graph of Section 6 takes about 1s on a standard laptop). This observation naturally opens some interesting questions:

- is the diffraction coefficient arising from Radlow's ansatz a very good far-field approximation, even in the region inaccessible by the MSF;
- why does the near-field have seemingly no influence on the far-field behaviour;
- can we find a constructive method for determining the function G_{+-} , and hence a unique formulation reconciling near-field and far-field;
- can we take a similar approach in the Neumann case?

We hope to be able to answer these points in our future work, several of which could have profound consequences on how we approach diffraction problems in general.

A Factorisation of $K_{-\circ}$ and $K_{+\circ}$

Let us show how the factorisation of $K_{-\circ}$ is obtained. The factorisation of $K_{+\circ}$ is obtained in a very similar way. Introduce the auxiliary function $\mathfrak{K}_{-\circ}$ as

$$\mathfrak{K}_{-\circ}(\alpha) = \kappa(k, \alpha_2) K_{-\circ}^2(\alpha) = \frac{\kappa(k, \alpha_2)}{\kappa(k, \alpha_2) - \alpha_1} = \frac{1}{1 - \frac{\alpha_1}{\kappa(k, \alpha_2)}}.$$

Naturally, for a given α_2 in \mathcal{A}_2 , $\mathfrak{K}_{-\circ}(\alpha)$ remains a *minus function* when seen as a function of α_1 . Plots of the auxiliary function $\mathfrak{K}_{-\circ}(\alpha)$ are provided in Figure 18.

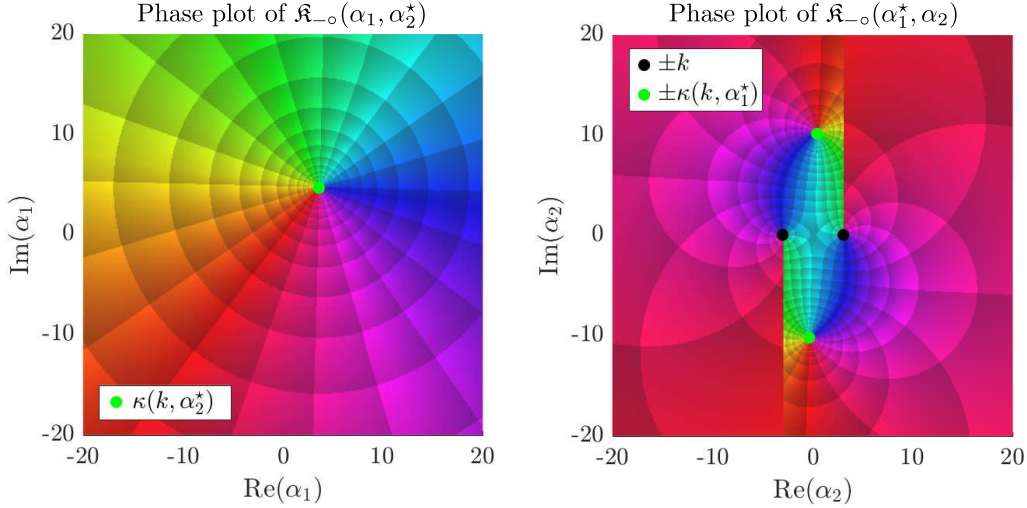


Figure 18: Left: Phase plot of the function $\mathfrak{K}_{-\circ}(\alpha_1, \alpha_2^*)$ for $\alpha_2^* = \mathcal{A}_2(5)$ in the α_1 complex plane. Right: Phase plot of the function $\mathfrak{K}_{-\circ}(\alpha_1^*, \alpha_2)$ for $\alpha_1^* = \mathcal{A}_1(10)$ in the α_2 complex plane.

Note that for $\mathfrak{K}_{-\circ}(\alpha_1, \alpha_2^*)$ (Figure 18, left) the point $\alpha_1 = \kappa(k, \alpha_2^*)$ is not a branch point anymore, but just a simple pole. For $\mathfrak{K}_{-\circ}(\alpha_1^*, \alpha_2)$ (Figure 18, right), as expected, $\alpha_2 = \pm k$ are branch points, while $\alpha_2 = \pm \kappa(k, \alpha_1^*)$ now correspond to two simple poles.

Let us now set $\alpha_1 \in \text{LHP}_1$. Now for a given α_2 in \mathcal{A}_2 (where $\mathfrak{K}_{-\circ}(\alpha)$ is analytic when considered as a function of α_2), we can make use of Corollary 4.1 to write $\mathfrak{K}_{-\circ}(\alpha) = \mathfrak{K}_{--}(\alpha) \mathfrak{K}_{-+}(\alpha)$, the equality being valid on $\mathcal{D}_{-\circ}$, where $\mathfrak{K}_{--}(\alpha)$ is analytic in LHP_2 and $\mathfrak{K}_{-+}(\alpha)$ is analytic in UHP_2 when both are considered as functions of α_2 . And, these are given by

$$\mathfrak{K}_{-+}(\alpha_1, \alpha_2) = e^{\frac{1}{2i\pi} \int_{\mathcal{A}_2^b} \frac{\check{\log}(\mathfrak{K}_{-\circ}(\alpha_1, z))}{z - \alpha_2} dz} \quad \text{and} \quad \mathfrak{K}_{--}(\alpha_1, \alpha_2) = e^{\frac{-1}{2i\pi} \int_{\mathcal{A}_2^a} \frac{\check{\log}(\mathfrak{K}_{-\circ}(\alpha_1, z))}{z - \alpha_2} dz},$$

where $\check{\log}$ was defined in Section 3.1. The choice of this particular logarithm is in fact extremely important in order to avoid crossings between branch cuts and the contour of integration. Using the exact expression of $\mathfrak{K}_{-\circ}(\alpha)$, this can be simplified to

$$\mathfrak{K}_{-+}(\alpha_1, \alpha_2) = e^{\frac{-1}{2i\pi} \int_{\mathcal{A}_2^b} \frac{\check{\log}\left(1 - \frac{\alpha_1}{\kappa(k, z)}\right)}{z - \alpha_2} dz} \quad \text{and} \quad \mathfrak{K}_{--}(\alpha_1, \alpha_2) = e^{\frac{1}{2i\pi} \int_{\mathcal{A}_2^a} \frac{\check{\log}\left(1 - \frac{\alpha_1}{\kappa(k, z)}\right)}{z - \alpha_2} dz}.$$

Going back to $K_{-\circ}(\alpha)$, we have

$$K_{-\circ}^2(\alpha) = \frac{\mathfrak{K}_{-\circ}(\alpha)}{\kappa(k, \alpha_2)} = \frac{\mathfrak{K}_{-+}(\alpha_1, \alpha_2) \mathfrak{K}_{--}(\alpha_1, \alpha_2)}{\sqrt[k]{k + \alpha_2} \sqrt[k]{k - \alpha_2}}.$$

Note that $\sqrt[4]{k + \alpha_2}$ is a *plus function* in the α_2 -plane (branch point at $\alpha_2 = -k$) and $\sqrt[4]{k - \alpha_2}$ is a *minus function* in the α_2 -plane (branch point at $\alpha_2 = +k$). Hence the function $\mathfrak{K}_{-+}/\sqrt[4]{k + \alpha_2}$ is a *plus function* and the function $\mathfrak{K}_{--}/\sqrt[4]{k - \alpha_2}$ is a *minus function*. We can then write $K_{-o}(\alpha) = K_{--}(\alpha)K_{-+}(\alpha)$, where $K_{--}(\alpha)$ is analytic in $\text{LHP}_1 \times \text{LHP}_2$ and $K_{-+}(\alpha)$ is analytic in $\text{LHP}_1 \times \text{UHP}_2$ when both are considered as functions of α_2 and given by

$$K_{-+}(\alpha) = \left(\frac{\mathfrak{K}_{-+}(\alpha_1, \alpha_2)}{\sqrt[4]{k + \alpha_2}} \right)^{1/2} = \frac{1}{\sqrt[4]{\sqrt[4]{k + \alpha_2}}} \exp \left\{ \frac{-1}{4i\pi} \int_{\mathcal{A}_\varepsilon^b} \frac{\overset{\vee}{\log} \left(1 - \frac{\alpha_1}{\kappa(k, z)} \right)}{z - \alpha_2} dz \right\}, \quad (\text{A.1})$$

and

$$K_{--}(\alpha) = \left(\frac{\mathfrak{K}_{--}(\alpha_1, \alpha_2)}{\sqrt[4]{k - \alpha_2}} \right)^{1/2} = \frac{1}{\sqrt[4]{\sqrt[4]{k - \alpha_2}}} \exp \left\{ \frac{1}{4i\pi} \int_{\mathcal{A}_\varepsilon^a} \frac{\overset{\vee}{\log} \left(1 - \frac{\alpha_1}{\kappa(k, z)} \right)}{z - \alpha_2} dz \right\}, \quad (\text{A.2})$$

recovering (4.4) and (4.5). This choice of realising the square root of the numerator by solely halving the inside of the exponential ensures that no spurious branch cuts occur. This would have been the case if instead we chose to take $\sqrt{}$ or even $\sqrt[4]{}$ of the numerator. The second square root of the denominator does not affect its branch cut structure. These functions are very fast to evaluate since the integrand now decays like x^{-2} along $\mathcal{A}_\varepsilon^a(x)$ as $x \rightarrow \pm\infty$.

B On the application of Liouville's theorem

B.1 A useful result

The following lemma is establishing a link between the decay of a function $\Phi(\alpha)$ and the decay of its respective plus and minus sum-split parts $\Phi_+(\alpha)$ and $\Phi_-(\alpha)$.

Lemma B.1 *Let $\Phi(\alpha)$ be a function analytic on some strip. And consider its sum-split $\Phi(\alpha) = \Phi_+(\alpha) + \Phi_-(\alpha)$, where Φ_+ and Φ_- are analytic in the UHP and LHP respectively.*

- a) *If $\Phi(\alpha) = \mathcal{O}(1/|\alpha|^\lambda)$ as $|\alpha| \rightarrow \infty$ within the strip, with $\lambda > 1$, then $\Phi_\pm(\alpha)$ are decaying at least like $1/|\alpha|$ as $|\alpha| \rightarrow \infty$ within their respective half-planes.*
- b) *If $\Phi(\alpha) = \mathcal{O}(1/|\alpha|)$ as $|\alpha| \rightarrow \infty$ within the strip, then $\Phi_\pm(\alpha)$ are decaying at least like $\ln|\alpha|/|\alpha|$ as $|\alpha| \rightarrow \infty$ within their respective half-planes.*
- c) *If $\Phi(\alpha) = \mathcal{O}(1/|\alpha|^\lambda)$ as $|\alpha| \rightarrow \infty$ within the strip, with $0 < \lambda < 1$, then $\Phi_\pm(\alpha)$ are decaying at least like $1/|\alpha|^\lambda$ as $|\alpha| \rightarrow \infty$ within their respective half-planes.*

These results are classic. The leading order results (as presented here) can be found for example in [40], while full asymptotic expansions are given in [23] and [39].

B.2 For the α_1 plane factorisation

Let us show that the top (resp. bottom) line of (5.6) tends to zero as $|\alpha_1| \rightarrow \infty$ within UHP_1 (resp. LHP_1), while $\alpha_2 \in \mathcal{A}_2$ is fixed. First of all, due to (5.3), it is clear that

$$G_{++}(\alpha_1, \alpha_2)/K_{-o}(a_1, \alpha_2) \stackrel{\alpha_2 \text{ fixed}}{\underset{|\alpha_1| \rightarrow \infty}{\sim}} \mathcal{O}(1/|\alpha_1|).$$

The condition on the $(x_1=0, x_2>0)$ edge implies that for a fixed $x_2>0$, for $x_3=0^+$, we have $\frac{\partial u}{\partial x_3} = \mathcal{O}(x_1^{-1/2})$ as $x_1 \rightarrow 0^+$, while $u = \mathcal{O}((-x_1)^{1/2})$ as $x_1 \rightarrow 0^-$. Because $F_{++} \propto \mathfrak{F}[\frac{\partial u}{\partial x_3}]$ and $G_{-+} = \mathfrak{F}[u_2]$ (see (5.2)), the Abelian theorems [25] imply that

$$F_{++} \stackrel{\alpha_2 \text{ fixed}}{\underset{|\alpha_1| \xrightarrow{\text{UHP}} \infty}{\sim}} \mathcal{O}(1/|\alpha_1|^{1/2}) \text{ and } G_{-+} \stackrel{\alpha_2 \text{ fixed}}{\underset{|\alpha_1| \xrightarrow{\text{LHP}} \infty}{\sim}} \mathcal{O}(1/|\alpha_1|^{3/2}). \quad (\text{B.1})$$

For a fixed $x_2<0$ and $x_3=0^+$, the field is well-behaved as $x_1 \rightarrow 0$, hence $u = \mathcal{O}(1)$. Since $G_{--} = \mathfrak{F}[u_3]$ and $G_{+-} = \mathfrak{F}[u_4]$, the Abelian theorems imply that

$$G_{+-} \stackrel{\alpha_2 \text{ fixed}}{\underset{|\alpha_1| \xrightarrow{\text{UHP}} \infty}{\sim}} \mathcal{O}(1/|\alpha_1|) \text{ and } G_{--} \stackrel{\alpha_2 \text{ fixed}}{\underset{|\alpha_1| \xrightarrow{\text{LHP}} \infty}{\sim}} \mathcal{O}(1/|\alpha_1|). \quad (\text{B.2})$$

Moreover we have

$$K_{+\circ}(\alpha_1, \alpha_2) \stackrel{\alpha_2 \text{ fixed}}{\underset{|\alpha_1| \rightarrow \infty}{\sim}} \mathcal{O}(1/|\alpha_1|^{1/2}) \text{ and } K_{-\circ}(\alpha_1, \alpha_2) \stackrel{\alpha_2 \text{ fixed}}{\underset{|\alpha_1| \rightarrow \infty}{\sim}} \mathcal{O}(1/|\alpha_1|^{1/2}). \quad (\text{B.3})$$

Hence, using (B.1), (B.2) and (B.3), we know that

$$F_{++} K_{+\circ} \stackrel{\alpha_2 \text{ fixed}}{\underset{|\alpha_1| \xrightarrow{\text{UHP}} \infty}{\sim}} \mathcal{O}\left(\frac{1}{|\alpha_1|}\right), \frac{G_{+-}}{K_{-\circ}} \stackrel{\alpha_2 \text{ fixed}}{\underset{|\alpha_1| \xrightarrow{\text{UHP}} \infty}{\sim}} \mathcal{O}\left(\frac{1}{|\alpha_1|^{1/2}}\right), \frac{G_{-\circ}}{K_{-\circ}} \stackrel{\alpha_2 \text{ fixed}}{\underset{|\alpha_1| \xrightarrow{\text{LHP}} \infty}{\sim}} \mathcal{O}\left(\frac{1}{|\alpha_1|^{1/2}}\right).$$

Finally, using the Lemma B.1c) in the α_1 plane, we conclude that we have (at least)

$$\left[\frac{G_{+-}}{K_{-\circ}}\right]_{+\circ} \stackrel{\alpha_2 \text{ fixed}}{\underset{|\alpha_1| \xrightarrow{\text{UHP}} \infty}{\sim}} \mathcal{O}\left(\frac{1}{|\alpha_1|^{1/2}}\right) \text{ and } \left[\frac{G_{+-}}{K_{-\circ}}\right]_{-\circ} \stackrel{\alpha_2 \text{ fixed}}{\underset{|\alpha_1| \xrightarrow{\text{LHP}} \infty}{\sim}} \mathcal{O}\left(\frac{1}{|\alpha_1|^{1/2}}\right).$$

This shows that the terms of the top (resp. bottom) line of (5.6) go to zero as $|\alpha_1| \rightarrow \infty$ within UHP₁ (resp. LHP₁). Hence, Liouville's theorem can safely be applied.

B.3 For the α_2 plane factorisation

Here we wish to show that E_{+2} tends to zero when α_1 is fixed in UHP₁ and $|\alpha_2| \rightarrow \infty$.

B.3.1 The terms without brackets

Let us show that the terms without brackets in the top line⁷ of (5.11) tend to zero as α_1 is fixed in UHP₁ and $|\alpha_2| \rightarrow \infty$ within UHP₂. First of all, using the expression (5.3) for G_{++} , it is straightforward to see that

$$\frac{G_{++}(\alpha)}{K_{--}(a_1, a_2) K_{+-}(\alpha_1, a_2)} \stackrel{\alpha_1 \text{ fixed}}{\underset{|\alpha_2| \rightarrow \infty}{\sim}} \mathcal{O}(1/|\alpha_2|). \quad (\text{B.4})$$

Moreover, using the definition of K_{++} and K_{-+} , we can see that

$$K_{++}(\alpha_1, \alpha_2) \stackrel{\alpha_1 \text{ fixed}}{\underset{|\alpha_2| \rightarrow \infty}{\sim}} \mathcal{O}(1/|\alpha_2|^{1/4}) \text{ and } K_{-+}(a_1, \alpha_2) \underset{|\alpha_2| \rightarrow \infty}{=} \mathcal{O}(1/|\alpha_2|^{1/4}).$$

The $(x_1>0, x_2=0)$ edge condition implies that for $x_3=0^+$ and a fixed $x_1>0$, $\frac{\partial u}{\partial x_3} = \mathcal{O}(x_2^{-1/2})$ as $x_2 \rightarrow 0^+$, which, by the Abelian theorems, requires that $F_{++}(\alpha_1, \alpha_2) = \mathcal{O}(1/|\alpha_2|^{1/2})$ for $\alpha_1 \in \text{UHP}_1$ as $|\alpha_2| \rightarrow \infty$ within UHP₂. This leads to

$$F_{++}(\alpha) K_{++}(\alpha) K_{-+}(a_1, \alpha_2) \stackrel{\alpha_1 \text{ fixed}}{\underset{|\alpha_2| \rightarrow \infty}{\sim}} \mathcal{O}(1/|\alpha_2|). \quad (\text{B.5})$$

⁷We can show in a very similarly fashion (omitted for brevity) that the terms without brackets in the bottom line of (5.11) do also tend to zero for fixed $\alpha_1 \in \text{UHP}_1$ and $|\alpha_2| \rightarrow \infty$ within LHP₂.

B.3.2 The terms with brackets

Because of Lemma B.1, in order to prove that the last term on the top (resp. bottom) line of (5.11) tends to zero as $|\alpha_2| \rightarrow \infty$ within UHP₂ (resp. LHP₂), it is sufficient to show that $\frac{K_{-+}(a_1, \alpha_2)}{K_{+-}} \left[\frac{G_{+-}}{K_{-o}} \right]_{+o}$ tends to zero as a power of $|\alpha_2|$ as $|\alpha_2| \rightarrow \infty$ while on \mathcal{A}_2 . In order to show this⁸, rewrite (5.9), which is valid for $\alpha_2 \in \mathcal{A}_2$, as

$$\frac{K_{-+}(a_1, \alpha_2)}{K_{+-}} \left[\frac{G_{+-}}{K_{-o}} \right]_{+o} = \underbrace{F_{++} K_{++} K_{-+}(a_1, \alpha_2)}_{\substack{\alpha_1 \text{ fixed} \\ |\alpha_2| \rightarrow \infty} \mathcal{O}(1/|\alpha_2|)} - \underbrace{\frac{G_{++}}{K_{--}(a_1, \alpha_2) K_{+-}}}_{\substack{\alpha_1 \text{ fixed} \\ |\alpha_2| \rightarrow \infty} \mathcal{O}(1/|\alpha_2|^{1/2})}.$$

The first estimate on the RHS is already given in the paper in (B.5), whilst the second comes naturally from the asymptotic behaviours

$$G_{++} \underset{|\alpha_2| \rightarrow \infty}{\overset{\alpha_1 \text{ fixed}}{=}} \mathcal{O}(1/|\alpha_2|), \quad K_{--} \underset{|\alpha_2| \rightarrow \infty}{\overset{\alpha_1 \text{ fixed}}{=}} \mathcal{O}(1/|\alpha_2|^{1/4}), \quad K_{+-} \underset{|\alpha_2| \rightarrow \infty}{\overset{\alpha_1 \text{ fixed}}{=}} \mathcal{O}(1/|\alpha_2|^{1/4}).$$

The first of these results is obvious given the exact expression (5.3) for G_{++} , whilst the second and third come directly from the integral representations (4.5) and (4.7). Hence, we have proved that the sufficient condition is satisfied and that, consequently, Liouville's theorem can safely be applied to obtain $E_{+2} \equiv 0$.

References

- [1] I. D. Abrahams. On the solution of Wiener-Hopf problems involving noncommutative matrix kernel decompositions. *SIAM J. Appl. Math.*, 57(2):541–567, 1997.
- [2] I. D. Abrahams, G. A. Kriegsmann, and E. L. Reiss. Sound radiation and caustic formation from a point source in a wall shear layer. *AIAA Journal*, 32(6):1135–1144, 1994.
- [3] M. Albani. On Radlow's quarter-plane diffraction solution. *Radio Sci.*, 42(6):1–10, oct 2007.
- [4] N Chr Albertsen. Diffraction by a quarterplane of the field from a halfwave dipole. *IEE Proc.-Microw. Antennas Propag.*, 144(3):191–196, 1997.
- [5] R. C. Assier and I. D. Abrahams. On the asymptotic properties of an interesting diffraction integral. [arXiv:2003.00237](https://arxiv.org/abs/2003.00237), 2020.
- [6] R. C. Assier and N. Peake. On the diffraction of acoustic waves by a quarter-plane. *Wave Motion*, 49(1):64–82, 2012.
- [7] R. C. Assier and N. Peake. Precise description of the different far fields encountered in the problem of diffraction of acoustic waves by a quarter-plane. *IMA J. Appl. Math.*, 77(5):605–625, 2012.
- [8] R. C. Assier, C. Poon, and N. Peake. Spectral study of the Laplace-Beltrami operator arising in the problem of acoustic wave scattering by a quarter-plane. *Q. J. Mech. Appl. Math.*, 69(3):281–317, 2016.

⁸Thank you to the anonymous reviewer for this suggestion!

- [9] R. C. Assier and A. V. Shanin. Diffraction by a quarter-plane. Analytical continuation of spectral functions. *Q. J. Mech. Appl. Math.*, 72(1):51–86, 2019.
- [10] V. M. Babich, D. B. Dement’ev, and B. A. Samokish. On the diffraction of high-frequency waves by a cone of arbitrary shape. *Wave Motion*, 21(3):203–207, may 1995.
- [11] V. M. Babich, D. B. Dement’ev, B. A. Samokish, and V. P. Smyshlyaev. On evaluation of the diffraction coefficients for arbitrary ”nonsingular” directions of a smooth convex cone. *SIAM J. Appl. Math.*, 60(2):536–573, feb 2000.
- [12] N. Bleistein. Saddle Point Contribution for an n -fold Complex-Valued Integral. <http://citeseerx.ist.psu.edu/viewdoc/download?doi=10.1.1.661.8737&rep=rep1&type=pdf>, 2012.
- [13] S. Blume. Spherical-multipole analysis of electromagnetic and acoustical scattering by a semi-infinite elliptic cone. *IEEE Antennas Propag. Mag.*, 38(2):33–44, apr 1996.
- [14] S. Bochner. A theorem on analytic continuation of functions in several variables. *Annals of Mathematics*, 39(1):14–19, 1938.
- [15] J. Boersma and J. K. M. Jansen. Electromagnetic field singularities at the tip of an elliptic cone, 1990.
- [16] R. V. Craster, A. V. Shanin, and E. M. Doubravsky. Embedding formulae in diffraction theory. *Proc. R. Soc. A*, 459(2038):2475–2496, oct 2003.
- [17] T. B. Hansen. Corner diffraction coefficients for the quarter plane. *IEEE Trans. Antennas Propag.*, 39(7):976–984, jul 1991.
- [18] J. B. Keller. Geometrical Theory of Diffraction. *J. Opt. Soc. Am.*, 52(2):116–130, 1962.
- [19] L. Kraus and L. M. Levine. Diffraction by an elliptic cone. *Commun. Pure Appl. Math.*, 14(1):49–68, 1961.
- [20] J. B. Lawrie and I. D. Abrahams. A brief historical perspective of the Wiener-Hopf technique. *J. Eng. Math.*, 59(4):351–358, oct 2007.
- [21] M. A. Lyalinov. Scattering of acoustic waves by a sector. *Wave Motion*, 50(4):739–762, jun 2013.
- [22] M. A. Lyalinov. Electromagnetic scattering by a plane angular sector : I . Diffraction coefficients of the spherical wave from the vertex. *Wave Motion*, 55:10–34, 2015.
- [23] J. P. McClure and R. Wong. Explicit error terms for asymptotic expansions of Stieltjes transforms. *J. Inst. Maths Applies*, 22:129–145, 1978.
- [24] E. Meister. Some solved and unsolved canonical problems of diffraction theory. *Lect. Notes Math.*, 1285:320–336, 1987.
- [25] B. Noble. *Methods Based on the Wiener-Hopf Technique for the Solution of Partial Differential Equations* . American Mathematical Society, 1988.
- [26] J. Radlow. Diffraction by a quarter-plane. *Arch. Ration. Mech. Anal.*, 8(2):139–158, 1961.

- [27] J. Radlow. Note on the diffraction at a corner. *Arch. Ration. Mech. Anal.*, 19:62–70, 1965.
- [28] R. Satterwhite. Diffraction by a quarter plane, exact solution, and some numerical results. *IEEE Trans. Antennas Propag.*, AP22(3):500–503, 1974.
- [29] A. V. Shanin. Coordinate equations for a problem on a sphere with a cut associated with diffraction by an ideal quarter-plane. *Q. J. Mech. Appl. Math.*, 58(Part 2):289–308, may 2005.
- [30] A. V. Shanin. Modified Smyshlyaev’s formulae for the problem of diffraction of a plane wave by an ideal quarter-plane. *Wave Motion*, 41(1):79–93, 2005.
- [31] A. V. Shanin. Asymptotics of waves diffracted by a cone and diffraction series on a sphere. *Journal of Mathematical Sciences*, 185(4):644–657, 2012.
- [32] V. P. Smyshlyaev. Diffraction by conical surfaces at high-frequencies. *Wave Motion*, 12(4):329–339, jul 1990.
- [33] V. P. Smyshlyaev. The high-frequency diffraction of electromagnetic waves by cones of arbitrary cross sections. *SIAM J. Appl. Math.*, 53(3):670–688, 1993.
- [34] A. Sommerfeld. Mathematische Theorie der Diffraction. *Mathematische Annalen*, 47(2-3):317–374, jun 1896.
- [35] A. Sommerfeld, R. J. Nagem, M. Zampolli, and G. Sandri. *Mathematical Theory of Diffraction (Progress in Mathematical Physics)*. Birkhauser, 2004.
- [36] M. Tew and R. Mittra. On a spectral domain approach for testing Albertsen’s corner diffraction coefficient. *Radio Science*, 15(3):587–594, 1980.
- [37] E. Wegert. *Visual Complex Functions*. Birkhauser Basel, 2012.
- [38] M. H. Williams. Diffraction by a finite strip. *Q. J. Mech. Appl. Math.*, 35:103–124, 1982.
- [39] R. Wong. Asymptotic expansion of the Hilbert transform. *SIAM J. Math. Anal.*, 11(1):92–99, 1980.
- [40] W.S. Woolcock. Asymptotic Behavior of Stieltjes transforms. I. *Journal of Mathematical Physics*, 8(6):1270–1275, 1967.